

# PARTITIONING THE PHENOTYPIC AND GENETIC VARIANCES OF REACTION NORMS

Pierre de Villemereuil<sup>1,2</sup> and Luis-Miguel Chevin<sup>3</sup>

<sup>1</sup>*Institut de Systématique, Évolution, Biodiversité (ISYEB), École Pratique des Hautes Études PSL, MNHN, CNRS, SU, UA, Paris, France*

<sup>2</sup>*Institut Universitaire de France (IUF)*

<sup>3</sup>*CEFE, CNRS, Université de Montpellier, Université Paul Valéry Montpellier 3, EPHE, IRD, Montpellier, France*

**Keywords:** phenotypic plasticity, quantitative genetics, character-state approach, polynomial approach, non-linear modelling

**Corresponding author:** Pierre de Villemereuil, E-mail: pierre.de-villemereuil@mnhn.fr

## Abstract

Many [<sup>1</sup>] traits show plastic phenotypic variation across environments, [<sup>2</sup>] captured by their norms of reaction. These reaction norms may be discrete or continuous, and can substantially vary in shape across organisms and traits, making it difficult to compare amounts and types of plasticity among ([<sup>3</sup>] or even within) studies. In addition, the evolutionary potential of phenotypic traits and their plasticity in heterogeneous environments critically depends on how reaction norms vary genetically, but there is no consensus on how this should be quantified. Here, we propose a partitioning of phenotypic variance across genotypes and environments that jointly address these challenges. We start by distinguishing the components of phenotypic variance arising from the average reaction norm across genotypes, [<sup>4</sup>] genetic variation in reaction norms (with additive and non-additive components), and a residual that cannot be predicted from the genotype and the environment. We then further partition the [<sup>5</sup>] genetic variance of the trait [<sup>6</sup>] (additive or not) into an environment-blind component and a component [<sup>7</sup>] arising from genetic variance in plasticity [<sup>8</sup>]. We show that the additive components can be expressed, and further decomposed according to the relative contributions from each parameter, using what we describe as the

---

<sup>1</sup>removed: phenotypic traits vary in a predictable way

<sup>2</sup>removed: as

<sup>3</sup>removed: and sometimes

<sup>4</sup>removed: (additive)

<sup>5</sup>removed: (additive)

<sup>6</sup>removed: into a component related the marginal (additive ) genetic variance in the trait

<sup>7</sup>removed: due to (additive)

<sup>8</sup>removed: , including for complex, non-linear reaction norms. The last step involves estimating contributions from different parameters of reaction norm shape to these variance components. This decomposition is general and we show how to apply it to various modelling approaches,

15 **reaction norm gradient. This allows for a very general framework applicable** from the character-state to  
16 curve-parameter approaches, including polynomial functions, or arbitrary non-linear models. To facilitate  
17 the use of this variance decomposition, we provide the Reacnorm R package, including a practical tutorial.  
18 Overall the toolbox we develop should serve as a [<sup>9</sup>]basis for an unifying and deeper understanding of  
19 the variation and genetics of reaction norms and plasticity, as well as more robust comparative studies of  
20 plasticity across organisms and traits.

## 21 Introduction

22 The phenotype of a given genotype can vary in response to its environment of development or expression,  
23 through a phenomenon broadly described as phenotypic plasticity (Schlichting & Pigliucci 1998; Bradshaw  
24 1965). Phenotypic plasticity is currently attracting considerable interest in the context of rapidly changing  
25 natural environments (Gienapp et al. 2008; Chevin et al. 2010; Merilä & Hendry 2014). While the mere exist-  
26 tence (and even prevalence) of phenotypic plasticity is uncontroversial, its relative contribution to observed  
27 or predicted phenotypic change in the wild (Teplitsky et al. 2008; Gienapp et al. 2008; Merilä & Hendry 2014;  
28 Bonamour et al. 2019), as well as the extent of its interplay with population-level processes such as natural se-  
29 lection and population dynamics (Reed et al. 2010; Vedder et al. 2013; Schaum & Collins 2014; de Villemereuil  
30 et al. 2020), are very active research areas. Answering these questions requires [<sup>10</sup>]biologists to be able  
31 to dissect and compare phenotypic plasticity in detail in a wide range of traits, environmental contexts and  
32 species. This requires a methodology that is appropriate for each context, while being general enough to be  
33 comparable across [<sup>11</sup>]contexts.

34 The relationship between the phenotype and the environment is captured by the reaction norm (or norm  
35 of reaction), which is defined at the level of genotypes (Woltereck 1909; Schlichting & Pigliucci 1998). Reaction  
36 norms encompass phenotypic responses to both continuous environments (such as temperature, salinity, etc.)  
37 and categorical/discrete ones (such as host plant for a phytophagous insect). Within a simple model of reaction  
38 norm, quantifying plasticity may be straightforward. For instance, both empirical (Charmantier et al. 2008;  
39 Nussey et al. 2005) and theoretical (Gavrilets & Scheiner 1993a; Lande 2009) work have extensively relied  
40 on the assumption of a linear reaction norm, whose slope is used as a metric of plasticity, since it quantifies  
41 how much phenotypic change is induced per unit environmental change. However, regression slopes are  
42 signed and have units of trait per environment, so even in this simple case some [<sup>12</sup>]standardisation is  
43 needed in order to compare the magnitude of plasticity among studies. Beyond this simple scenario, drawing  
44 robust conclusions about phenotypic plasticity requires being able to quantify and compare its magnitude

---

<sup>9</sup>removed: base

<sup>10</sup>removed: for

<sup>11</sup>removed: context

<sup>12</sup>removed: standardization

45 across organisms, traits and environments, in a way that is applicable across the statistical frameworks used  
46 to study plasticity.

47 Beyond *how much* phenotypes change with the environment, *how* they change can also be of importance.  
48 First, different reaction norm shapes may come with different biological interpretations. For instance, a bell-  
49 shaped (eg quadratic, Gaussian) reaction norm may indicate that some mechanism underlying a measured  
50 trait is maximized at an intermediate value of the environment. This is often expected for traits that are direct  
51 components of fitness, or that can be interpreted as proxys for performance, for which the reaction norms  
52 are generally termed tolerance or performance curves (Lynch & Gabriel 1987; Deutsch et al. 2008; Angilletta  
53 2009). A sigmoid shape, on the other hand, may indicate that plasticity is directional but that the range of  
54 possible phenotypes is constrained, or that selection favors discrete-like variation (Moczek & Emlen 1999;  
55 Suzuki & Nijhout 2006; Hammill et al. 2008; Chevin et al. 2013). Second, most theoretical models on the  
56 evolution of plasticity, especially those based on quantitative genetics which are most directly comparable to  
57 empirical data, assume a given reaction norm shape - often linear for simplicity (Scheiner 1993b; Tufto 2000;  
58 Lande 2009). The extent to which theoretical predictions on the evolution of plasticity apply to any particular  
59 empirical system thus depends on how well the reaction norm shape assumed in the models conforms to  
60 observations in this system. In other words, we need some metric for whether a reaction norm is "mostly  
61 linear" or "mostly curved", for instance. In addition, when fitting a particular model of reaction norm shape  
62 to an empirical dataset, we would like to know how well this model captures the overall plastic variation of  
63 the trait across environments.

64 A third crucial question regarding reaction norms is how (and how much) they vary genetically. It has  
65 long been recognized that plasticity can evolve if reaction norms vary genetically (Bradshaw 1965), and theory  
66 has predicted how different aspects of reaction norm shape are expected to respond to selection in a variable  
67 environment (de Jong 1990; Gomulkiewicz & Kirkpatrick 1992; Gavrillets & Scheiner 1993a). However this  
68 theory has been little applied empirically, except for predictions about the slope of linear reaction norms (or  
69 phenotypic differences between two environments). But beyond this, it should also be of interest to identify  
70 which aspects of reaction norm shape are more likely to evolve, based on how they vary genetically. For  
71 instance, a reaction norm may be highly curved (e.g. quadratic) but have little genetic variability in curvature,  
72 instead mostly varying in position, height, or local slope. Distinguishing between the genetic variance of the  
73 trait, marginalised across environments, and the genetic variance of plasticity itself, can also be a conceptual  
74 and methodological challenge. There is thus a need to compare genetic variation in different components of  
75 reaction norm, but previous attempts to do so (in a meta-analysis) were limited by methodological obstacles  
76 (Murren et al. 2014, see the Appendix). In fact, comparing genetic variation in the slope versus curvature  
77 of a reaction norm, for instance, is not straightforward, as these parameters have different scales and even

78 units (trait per environment, vs trait per squared environment). [<sup>13</sup>] Moreover, even the notion of average  
79 slope and curvature can have different meanings depending on the assumed distribution for the environment.  
80 Genetic variation in reaction reaction norm shape can be analyzed by estimating variation in the parameters  
81 of a continuous function of the environment, as done by the flexible framework of function-valued traits  
82 (Kirkpatrick & Heckman 1989; Gomulkiewicz & Kirkpatrick 1992; Stinchcombe et al. 2012). In addition, it  
83 would be useful to be able to compare the relative contributions of variation in different aspects of reaction  
84 norm shape to the overall variance [<sup>14</sup>] arising from plasticity of a trait.

85 We herein propose a theoretically justified and generally applicable framework to estimate and partition  
86 the phenotypic variance of reaction norms, towards three main goals: (i) quantify the contribution of plasticity  
87 to the total phenotypic variance in reaction norms; (ii) evaluate the contribution of different aspects of reaction  
88 norm shape, and of the full assumed reaction norm model, to overall plastic phenotypic variation; and (iii)  
89 quantify heritable variation in the trait and its [<sup>15</sup>] plastic component, due to the different aspects of the  
90 reaction norm. We provide this framework as a new R package Reacnorm, including a tutorial to guide users  
91 in applying it. Our hope is that this will stimulate more quantitative investigations of the ways in which  
92 phenotypic plasticity contributes to phenotypic variation and evolutionary change.

## 93 Reaction norm models

94 In the broadest sense, a reaction norm is a decomposition of phenotypic variation among known (often con-  
95 trolled) versus unknown sources of environmental variation. In this sense, we can start by decomposing the  
96 phenotypic trait  $z$  into two components:

$$z = \hat{z} + \tilde{z}. \quad (1)$$

97 The first term  $\hat{z}$  is the reaction norm, that is, the component of phenotypic variation that can be predicted  
98 (hence the hat notation) from knowing both the genotype (which we will note  $g$  throughout) of an individual  
99 and the environment (which we will note  $\epsilon$  throughout) in which it developed. Note that by “environment”, we  
100 mean either an experimentally controlled environmental variable, or a focal variable (e.g. temperature) within  
101 a naturally occurring environmental context. The second term  $\tilde{z}$  is the component of the measured phenotype  
102 that cannot be predicted from genotype and environment, and arises from unknown environmental factors  
103 (usually described as micro-environmental variation), developmental noise, and measurement error.

104 Types of reaction norms  $\hat{z}$  can be further categorised according to the type of environmental variation.  
105 The environment may be inherently categorical and unordered, such as host plant for a herbivore insect. It

---

<sup>13</sup>removed: More

<sup>14</sup>removed: in

<sup>15</sup>removed: plasticity

**Table 1:** List of the main notations, as well as their source of variation. We here distinguish the “focal” environment, which only concerns the environmental variable used to parametrise the reaction norm, from other putative sources of environmental variation that may influence the phenotypic trait (sometimes described as micro-environmental variation). “Everything” in the table thus includes all (focal and other) sources of environmental and genetic variation, developmental noise and measurement error.

Notation	Explanation	Varies over
$z$	Phenotypic value for the trait	Everything
$\hat{z}$	Phenotype as predicted from the environment and the genotype	Focal environment, genotypes
$\varepsilon$	Environmental variable	—
$\boldsymbol{\mu}$	Vector of the average value of the phenotypic in each environment	Focal environment
$G_z$	Additive genetic variance-covariance matrix of trait values across environments (character states)	—
$\boldsymbol{\theta}_g$	Vector of parameter values of the reaction norm for genotype $g$	Genotypes
$\bar{\boldsymbol{\theta}}$	Vector of mean values of the reaction parameters over the genotypes	—
$G_{\boldsymbol{\theta}}$	Additive genetic variance-covariance matrix of the reaction norm parameters	—
$\boldsymbol{\psi}_{\varepsilon}$	Reaction norm gradient, the vector of partial derivatives of the phenotype $z$ against reaction norm parameters $\boldsymbol{\theta}_g$ , averaged over the genotypes at environment $\varepsilon$	Focal environment
$\Psi$	Variance-covariance matrix of $\boldsymbol{\psi}_{\varepsilon}$ across environments	—
$V_p$	Total phenotypic variance in the trait $z$	—
$V_{\text{Res}}$	Residual variance, not explained by the reaction norm	—
$V_{\text{Plas}}, P_{\text{RN}}^2$	Phenotypic variance arising from changes in the mean reaction norm across environments; divided by $V_p$ for $P_{\text{RN}}^2$	—
$V_{\text{Gen}}, H_{\text{RN}}^2$	Total genetic variance in the trait across environments; divided by $V_p$ for $H_{\text{RN}}^2$	—
$V_{\text{Add}}, h_{\text{RN}}^2$	Total additive genetic variance in the trait across environments; divided by $V_p$ for $h_{\text{RN}}^2$	—
$V_A, h^2$	[.. <sup>a</sup> ]Environment-blind additive genetic variance of the trait, i.e. based on the mean breeding values across environments, divided by $V_p$ for $h^2$	—
$V_{A \times E}, h_1^2$	Additive genetic variance [.. <sup>b</sup> ]arising from plasticity, i.e. variance of the mean-centred breeding values, divided by $V_p$ for $h_1^2$	—
$\pi_{\text{Sl}}, \pi_{\text{Cv}}$	Proportion of $V_{\text{Plas}}$ explained by the average slope ( $\pi_{\text{Sl}}$ ) or curvature ( $\pi_{\text{Cv}}$ ) of the average reaction norm	—
$\varphi_i, \varphi_{ij}$	Proportion of $V_{\text{Plas}}$ explained by parameter $i$ , or by covariation between parameter $i$ and $j$ for a polynomial reaction norm	—
$\gamma_i, \gamma_{ij}$	Proportion of $V_{\text{Add}}$ explained by the additive genetic (co)variation in parameter $i$ (and $j$ )	—
$l_i, l_{ij}$	Proportion of $V_{A \times E}$ explained by the additive genetic (co)variation in parameter $i$ (and $j$ )	—

<sup>a</sup>removed: Marginal

<sup>b</sup>removed: in

106 may be ordered but with no (or unknown) quantitative value, such as low, medium, and high treatments. Or  
 107 it may be ordered quantitatively, with values that are either intrinsically discrete, such as habitat quality, or  
 108 continuous, such as temperature or salinity.

109 When environments are categorical, the reaction norm can be studied by treating phenotypic values in  
 110 different environments as alternative ‘character states’, considered as different traits in a multivariate frame-

111 work (Via & Lande 1985; Falconer 1952). The mean character state may differ among [<sup>16</sup>]environments if  
 112 the trait is plastic; phenotypic and genetic variation may be larger in some environments; and phenotypes  
 113 may be more or less correlated across environments (Via & Lande 1985; Falconer 1952). Such a modelling  
 114 framework is readily described by Equation 1 for a genotype  $g$  and environment  $\varepsilon_k$  (where the index  $k$  is used  
 115 to reflect the discrete aspect of the environmental variable). In practice, such an approach would correspond  
 116 to an ANOVA (or a mixed model) with discrete environment and genotype-within-environment as (random)  
 117 effects of the model. In its most compact form, such a statistical model can be framed as a multivariate Gaus-  
 118 sian distribution, with [<sup>17</sup>]the number of dimensions corresponding to the number of categories in the  
 119 environment,

$$\hat{z} \sim \mathcal{N}(\boldsymbol{\mu}, G_z), \quad (2)$$

120 where  $\boldsymbol{\mu}$  is the vector of expected phenotypic values (across genotypes) within each environment, and  $G_z$  is  
 121 the genetic variance-covariance matrix of trait values within and across environments. [<sup>18</sup>][<sup>19</sup>]

122 For quantitative environments (both discrete and continuous), the most common approach is to model  
 123 the reaction norm as a function of environment and genotype:

$$\hat{z} = f(\varepsilon, \boldsymbol{\theta}_g), \quad (3)$$

124 where  $\varepsilon$  is the environmental value, and  $\boldsymbol{\theta}_g$  is a vector that contains the parameters of the function (e.g. coeffi-  
 125 cients associated to each exponent for a polynomial) for each genotype  $g$ ; these parameters are thus genetically  
 126 variable. The parameters  $\boldsymbol{\theta}_g$  are generally assumed to be polygenic and thus follow a multivariate Gaussian  
 127 distribution,

$$\boldsymbol{\theta}_g \sim \mathcal{N}(\bar{\boldsymbol{\theta}}, G_\theta), \quad (4)$$

128 where  $\bar{\boldsymbol{\theta}}$  is the vector of average parameter values across genotypes and  $G_\theta$  is the additive genetic variance-  
 129 covariance matrix of the parameters  $\boldsymbol{\theta}_g$ . This approach has been described alternatively as the “reaction  
 130 norm” approach, the “polynomial approach”, or a parametric version of function-valued traits. To keep it  
 131 general here and avoid confusion with the general concept of reaction norm as defined in Equation 1 (which  
 132 applies even to categorical environments), we will describe it as the “curve-parameter” approach. Note that  
 133 Equation 4 assumes that the only source of variation in reaction norm parameters  $\boldsymbol{\theta}$  is genetic. In cases where  
 134 reaction norms can be measured in individuals using repeated measurements across environments (individual

---

<sup>16</sup>removed: environment

<sup>17</sup>removed: a

<sup>18</sup>removed: Note that when the environment is quantitative but discrete, one may still use the character-state approach, but structuring correlations in  $G_z$  by environmental distance, in effect treating the phenotype as a stochastic process characterized by its autocovariance function across environments

<sup>19</sup>removed: .

135 plasticity *sensu* Nussey et al. 2007) it can be necessary, or useful, to include other sources of variation in  $\theta$ ,  
 136 including confounding environmental effects, or permanent environmental effects. For the sake of simplicity,  
 137 we will assume throughout that all variation in  $\theta$  is genetic, but we show in Appendix C5 that relaxing this  
 138 assumption only affects how non-genetic variances are computed.

139 It can be shown that the character-state and curve-parameter approaches are equivalent, following the  
 140 spirit of de Jong (1995), who showed that a polynomial curve of sufficient order is exactly equivalent to a  
 141 character-state model. In particular, the character-state in Equation 2 can be expressed using Equation 3 and  
 142 Equation 4 by letting  $\bar{\theta} = \mu$ ,  $G_\theta = G_z$  and  $f$  a function that outputs the  $k$ th value of  $\theta_g$  when evaluated at  
 143  $\varepsilon_k$  environment (see Appendix A). In the following, we will derive general results using the more general  
 144 formalism of Equation 3 and Equation 4, and then express them for the particular case of the character-state  
 145 approach when relevant.

## 146 Partitioning variation in reaction norms

### 147 Complete partition of the variation in reaction norms

148 The total phenotypic variance in the reaction norm can be partitioned by isolating independent components  
 149 of variation. The main reasoning will be summarised here, with more mathematical details provided in the  
 150 Appendix A to Appendix D. For a start, the terms in Equation 1 are assumed to be independent, such that  
 151 the total phenotypic variance  $V(z)$  (usually noted  $V_P$ ) is the sum of the variance predicted by the genotype  
 152 and the environment  $V(\hat{z})$ , plus a residual component of variance  $V(\tilde{z}_i)$ , which we will note  $V_{Res}$ . Then, a  
 153 second distinction can be made between the general, average shape of the reaction norm, and the genotype-  
 154 specific variation surrounding such an average, as illustrated in Figure 1 using a quadratic reaction norm. The  
 155 component of phenotypic variance arising from plastic responses to the environment by the mean reaction  
 156 norm, i.e. after averaging across all genotypes (Figure 1), will be denoted  $V_{Plas}$ . This variance can be considered  
 157 as fully ascribed to the environmental component of phenotypic variation. The component of phenotypic  
 158 variation attributable to genetic variation in the reaction norm Figure 1 will be denoted  $V_{Gen}$ . As these two  
 159 components are independent by construction, denoting as  $E_{g|\varepsilon}(\hat{z})$  the expected value of the reaction norm  
 160 across genotypes at a given environmental value  $\varepsilon$ , we have

$$V(\hat{z}) = V(E_{g|\varepsilon}(\hat{z})) + V(\hat{z} - E_{g|\varepsilon}(\hat{z})) = V_{Plas} + V_{Gen}, \quad (5)$$

161 such that

$$V_P = V_{Plas} + V_{Gen} + V_{Res}. \quad (6)$$

162 Compared to the classical equation  $V_P = V_G + V_E + V_{G \times E}$  (Falconer & Mackay 1996; Lynch & Walsh 1998;  
 163 Des Marais et al. 2013), the correspondence is that  $V_E = V_{Plas} + V_{Res}$  and  $V_{Gen} = V_G + V_{G \times E}$ . Also note that both  
 164 decompositions make the same common assumption that genotypes and environments are not correlated.  
 165 We have thus decomposed the environmental variance into a component due to phenotypic plasticity in  
 166 response to  $\varepsilon$  ( $V_{Plas}$ ) on the one hand, and any other residual source of phenotypic variation ( $V_{Res}$ ) on the other  
 167 hand, as commonly done in theory (Via & Lande 1985; Gavrillets & Scheiner 1993a) as well as in practice.

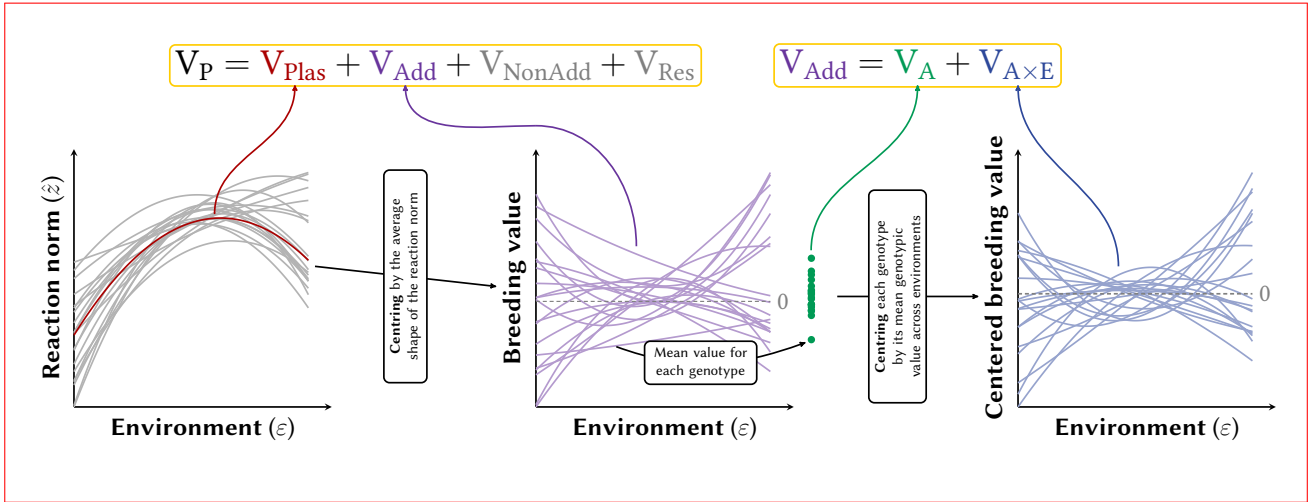


**Figure 1:** Illustration of the full variance decomposition using quadratic reaction norms. We start from the reaction norms (left graph, grey lines, the residual variance is not illustrated) and compute their average shape across all genotypes (left graph, red line). The phenotypic variance arising from this average shape is  $V_{Plas}$ . Centering the reaction norms along this average shape directly yields the distribution of the breeding values along environments (middle graph, purple lines), because in this quadratic case, the non-additive genetic variance is  $V_{NonAdd} = 0$ . The total variance of the breeding values along the environment is  $V_{Add}$ . The classical, environment-blind additive genetic variance  $V_A$  is the variance of the breeding values averaged across environments for each genotype (middle graph, green dots). The  $V_{A \times E}$  is the variance of the remainder of the breeding values after mean-centering (right graph, blue lines).

168 The genotypic variance  $V_{Gen}$  accounts for all sources of genetic variation, including the genotype-by-  
 169 environment interaction. Note that this contrasts with a view where the genotype-by-environment interac-  
 170 tion is instead associated with the environmental component, e.g. as *plastic variance* (Scheiner & Lyman 1989;  
 171 Scheiner 1993a; Falconer & Mackay 1996; Lynch & Walsh 1998).

172 [..<sup>20</sup>]

173 [..<sup>21</sup>]As seen above,  $V_{Gen}$  can be [..<sup>22</sup>]decomposed into the genetic variance of the trait, measured using its  
 174 average genotypic value across environments ( $V_G$ ), and the variance arising from genotype-by-environment  
 175 interaction ( $V_{G \times E}$ ). Here, we will apply such decomposition at the level of the additive genetic variance ( $V_{Add}$ ),

<sup>20</sup>removed: Illustration of the full variance decomposition using quadratic reaction norms. We start from the reaction norms (left graph, grey lines, the residual variance is not illustrated) and compute its average shape across all genotypes (left graph, red line). The phenotypic variance arising from this average shape is  $V_{Plas}$ . Centering the reaction norms along this average shape directly yields the distribution of the breeding values along environments (middle graph, purple lines), because in this quadratic case, the non-additive genetic variance is  $V_{NonAdd} = 0$ . The total variance of the breeding values along the environment is  $V_{Add}$ . The classical, average additive genetic variance  $V_A$  is the variance of the average of the breeding values across the environments for each genotype (middle graph, green dots). The  $V_{A \times E}$  is the variance of the remainder of the breeding values after mean-centering (right graph, blue lines).

<sup>21</sup>removed: The genotypic variance

<sup>22</sup>removed: further decomposed in two steps. First, we can isolate the *additive* genetic variance ( $V_{Add}$ ), from the *non-additive*



176 relegating all the non-additive parts of  $V_G$  and  $V_{G \times E}$  into a common  $V_{\text{NonAdd}}$  [<sup>23</sup>] component (Figure 1), arising from dominance and epistasis (Lynch & Walsh 1998; Falconer & Mackay 1996). Usually, models like Equation 2 or Equation 4 are defined using additive genetic variance-covariance matrices for their basic parameters, meaning that  $V_{\text{Add}}$  can be directly estimated from the models. As such, we will discard explicit inclusion of dominance or epistasis variance components in a theoretical or statistical model throughout, for the sake of simplicity. However, non-additive genetic variance can still arise from non-linearity in the (assumed) developmental system (Rice 2004; Morrissey 2015; de Villemereuil et al. 2016; de Villemereuil 2018), meaning that non-additive variance can be generated by the reaction norm itself. Looking at Equation 3 and Equation 4, the ultimate source of any additive genetic variation in the trait  $z$  comes from the additive genetic variation in the parameters  $\theta$ . As a result, non-additivity in the trait arises when the function  $f(\varepsilon, \theta)$  in Equation 3 is non-linear with regard to  $\theta$ , a situation we will refer to as “non-linearity in the parameters”. Importantly, this means that polynomial (e.g. quadratic) functions, which are linear in their parameters, are such that  $V_{\text{NonAdd}} = 0$  and  $V_{\text{Gen}} = V_{\text{Add}}$ .

189 When studying the evolution of plasticity, it proves useful to further decompose  $V_{\text{Add}}$  into two components. The first is the [<sup>24</sup>] environment-blind additive genetic variance of the trait, arising from differences in average breeding values between genotypes, and typically equal to the classical  $V_A$ . In other words,  $V_A$  is the variance of the breeding values after averaging them across environments (Figure 1), as would be obtained if the genotype-by-environment interaction was ignored altogether. For example, it would be the output of a simple animal model analysis of repeated measurements of a plastic trait in a wild population. The second component of  $V_{\text{Add}}$  is the additive genetic variance [<sup>25</sup>] arising from plasticity, which we will note  $V_{A \times E}$  (for additive genetic component due to genotype-by-environment interactions).  $V_{A \times E}$  is the remaining additive genetic variance in the reaction norm after removing the mean breeding value for each genotype (Figure 1). This definition is akin to the one used by Albecker et al. (2022), but here more directly expressed in terms of variance of breeding values, i.e. additive genetic variance. It measures the potential for evolution of plasticity in the trait. Notably, if  $V_{A \times E} = 0$  but  $V_{\text{Add}} > 0$ , then the additive genetic variation in the reaction norms is only due to average differences between genotypes, i.e. the reaction norms of different genotypes are parallel. The variances  $V_A$  and  $V_{A \times E}$  are exactly equivalent to the classical decomposition using  $V_G$  and  $V_{G \times E}$ , only applied to the heritable part of the genetic variance. We show below that it is possible to express  $V_{\text{Add}}$ ,  $V_A$  and  $V_{A \times E}$  in a way that encompasses all approaches of reaction norm, from a character-state to a curve that is non-linear in its parameters, by computing reaction norm gradients of the trait  $z$  with respect to its reaction norm parameters  $\theta$ , in line with previous theoretical results for the quantitative genetics of

---

<sup>23</sup>removed: )

<sup>24</sup>removed: marginal

<sup>25</sup>removed: of

207 non-linear developmental systems and non-Gaussian traits (Morrissey 2015; de Villemereuil et al. 2016),.

208 The complete partition of the phenotypic variance is thus:

$$V_P = V_{\text{Plas}} + V_A + V_{A \times E} + V_{\text{NonAdd}} + V_{\text{Res}}. \quad (7)$$

209 From this, it is possible to derive unitless quantities of interest, for instance by standardising by the pheno-  
210 typic variance, **which is more widely applicable and appropriate than mean-standardisation in the context**  
211 **of reaction norms** (Pélabon et al. 2020). In particular:

$$P_{\text{RN}}^2 = \frac{V_{\text{Plas}}}{V_P}, \quad (8)$$

212 is the proportion of the phenotypic variance arising from average plastic responses to environments (depend-  
213 ing on the average reaction norm shape). Variance-standardised additive genetic variances are heritabilities.  
214 In our case, we can use  $V_{\text{Add}}$ ,  $V_A$  or  $V_{A \times E}$  as the numerator, yielding the following relationship:

$$h_{\text{RN}}^2 = \frac{V_{\text{Add}}}{V_P} = \frac{V_A}{V_P} + \frac{V_{A \times E}}{V_P} = h^2 + h_I^2. \quad (9)$$

215 In other words, the heritability of the trait when fully accounting for its reaction norm ( $h_{\text{RN}}^2$ ) is equal to the  
216 **[..<sup>26</sup>]environment-blind** heritability of the trait ( $h^2$ , based on the **[..<sup>27</sup>]breeding values averaged** across envi-  
217 ronments) plus the heritability **[..<sup>28</sup>]from plasticity** (**[..<sup>29</sup>]  $h_I^2$ , based on the breeding values by environment**  
218 **interaction**). If it is not possible to measure additive genetic variances due to limitations in the experimental  
219 design (e.g. when “genotypes” correspond to populations, accessions or clones), it is possible to perform the  
220 same decomposition using “broad-sense heritabilities”,

$$H_{\text{RN}}^2 = \frac{V_{\text{Gen}}}{V_P} = \frac{V_G}{V_P} + \frac{V_{G \times E}}{V_P} = H^2 + H_I^2. \quad (10)$$

221 In all cases, the quantity:

$$T_{\text{RN}}^2 = \frac{V_{\text{Plas}} + V_{\text{Gen}}}{V_P} = P_{\text{RN}}^2 + H_{\text{RN}}^2 \quad (11)$$

222 would measure the proportion of the phenotypic variance explained by the (possibly plastic and genetically  
223 variable) reaction norm, and thus our ability to predict the individual phenotype from the genotype and  
224 the environment. In a linear context with respect to the parameters, when the environment is considered a  
225 fixed quantity, the quantities  $P_{\text{RN}}^2$  and  $T_{\text{RN}}^2$  are analogous to the (resp. marginal and conditional) coefficient of

---

<sup>26</sup>removed: marginal

<sup>27</sup>removed: averaged breeding values

<sup>28</sup>removed: of plasticity, arising from interaction with the environment

<sup>29</sup>removed:  $h_I^2$

226 determination of the reaction norm (Nakagawa & Schielzeth 2013; Johnson 2014), but their definition here is  
 227 given beyond that simple context. Relaxing the assumption that the only source of variation in  $\theta$  is of genetic  
 228 origin (e.g. individual plasticity, Nussey et al. 2007), we show in Appendix C5 that only the computation of  
 229  $V_P$  and  $T_{RN}^2$  are slightly affected.

230 Importantly, so far we are not making any statement about the actual reaction norm shape:  $P_{RN}^2$  captures  
 231 the contribution of the average reaction norm regardless of its shape, and the broad- or narrow-sense heritabil-  
 232 ities the contribution of various aspects the genetic variation to the phenotypic variance. The contribution  
 233 of detailed aspects of reaction norms shape to phenotypic variation are obtained by further partitioning  $V_{Plas}$   
 234 and the additive genetic variances, as we do below.

## 235 Contributions of reaction norm shape and parameters to the plastic 236 variance

237 As stated in Equation 5, the general definition of the variance arising from the average reaction norm is  
 238  $V_{Plas} = V(E_{g|\varepsilon}(\hat{z}))$ . Important simplifications arise in more particular cases. For example, when the assumed  
 239 curve is linear in its parameters,  $E_{g|\varepsilon}(\hat{z}) = f(\varepsilon, \bar{\theta})$ , where  $\bar{\theta}$  is the average value of the parameters across  
 240 genotypes. In particular, in the case of a quadratic reaction norm (Scheiner 1993a; Gavrillets & Scheiner  
 241 1993b; Morrissey & Liefting 2016):

$$f(\varepsilon, \theta_g) = (\bar{a} + a_g) + (\bar{b} + b_g)\varepsilon + (\bar{c} + c_g)\varepsilon^2, \quad (12)$$

242 where  $\bar{a}$ ,  $\bar{b}$ ,  $\bar{c}$  are the average intercept, first- and second-order parameters of the model, and  $a_g$ ,  $b_g$  and  $c_g$  are  
 243 genotype-specific deviation from these average values for the same parameters, we can express  $V_{Plas}$  simply  
 244 as:

$$V_{Plas} = \bar{b}^2 V(\varepsilon) + \bar{c}^2 V(\varepsilon^2) + 2\bar{b}\bar{c}\text{cov}(\varepsilon, \varepsilon^2). \quad (13)$$

245 If the environmental variable  $\varepsilon$  has been mean-centred and is symmetrical, then  $\text{cov}(\varepsilon, \varepsilon^2) = 0$  and the third  
 246 term vanishes. Finally, in the case of a character-state model, the average phenotype in each environment  
 247  $\varepsilon_k$  is readily provided by the  $\mu_k$  in Equation 2, so that  $V_{Plas} = V(\mu)$ . Once  $V_{Plas}$  is computed, its standardised  
 248 version  $P_{RN}^2$  follows by dividing by the total phenotypic variance.

249 Pushing the analysis further, we aim to compute the contributions of different aspect of reaction norm  
 250 shape to the overall environmental plastic variance of the trait, notably the contribution of its slope and  
 251 curvature, which we will denote as  $\pi_{SI}$  and  $\pi_{CV}$ , respectively. For this, at least one of two of the following  
 252 assumptions must be valid: (i)  $\varepsilon$  follows a normal distribution, or (ii) the true reaction norm is quadratic. In  
 253 all cases, it also require that the environmental variable has been mean-centered. A last requirement is for  $f$

254 to be at least twice differentiable with respect to  $\varepsilon$  (which excludes e.g. the character-state approach). In this  
 255 case, these terms simply depend on the average first- and second-order derivative of  $E_{g|\varepsilon}(\hat{z})$  and the variance  
 256 of  $\varepsilon$  and  $\varepsilon^2$  (see [Appendix D1](#)):

$$\pi_{\text{Sl}} = \frac{E\left(\frac{dE_{g|\varepsilon}}{d\varepsilon}(\hat{z})\right)^2 V(\varepsilon)}{V_{\text{Plas}}}, \quad \pi_{\text{Cv}} = \frac{\frac{1}{4}E\left(\frac{d^2E_{g|\varepsilon}}{d\varepsilon^2}(\hat{z})\right)^2 V(\varepsilon^2)}{V_{\text{Plas}}}. \quad (14)$$

257 An important point arising from [Equation 14](#) is that the relative importance of variation in the slope and cur-  
 258 vature components of reaction norm depend on variation in the environment, respectively  $V(\varepsilon)$  and  $V(\varepsilon^2)$   
 259 (note that  $V(\varepsilon^2) = 2V(\varepsilon)^2$  if the environment is normally distributed). Crucially, we chose to express this  
 260 partitioning using the mean environment as the reference environment (as commonly practiced, e.g. Morris-  
 261 sey & Liefing [2016](#)), but any other choice of a reference environment would result in a different  $\pi$ -partition,  
 262 notably due to a non-null value for  $\text{Cov}(\varepsilon, \varepsilon^2)$ . Fortunately, neither  $V_{\text{Plas}}$  nor  $P_{\text{RN}}^2$  are impacted by this choice  
 263 in the reference environment. Furthermore, if the reaction norm is linear [[..<sup>30</sup>](#)] in the parameters, the deriva-  
 264 tives of  $E_{g|\varepsilon}(\hat{z})$  can be directly taken as the derivatives of  $f$ . In particular, for a quadratic reaction norm as in  
 265 [Equation 12](#), for a mean-centred environment, those quantities simply are:

$$\pi_{\text{Sl}} = \frac{\bar{b}^2 V(\varepsilon)}{V_{\text{Plas}}}, \quad \pi_{\text{Cv}} = \frac{\bar{c}^2 V(\varepsilon^2)}{V_{\text{Plas}}}, \quad (15)$$

266 consistent with the fact the first and second order coefficients of a quadratic polynomial correspond to its  
 267 average slope and curvature, respectively. Only in this configuration do we have  $\pi_{\text{Sl}} + \pi_{\text{Cv}} = 1$ . Unfortunately,  
 268 this simple, geometric interpretation of the polynomial coefficients is lost above the second-order case (see  
 269 [Appendix D](#)).

270 [Figure 2](#) shows the values of  $\pi_{\text{Sl}}$  and  $\pi_{\text{Cv}}$  for various quadratic reaction norms, assuming  $\varepsilon$  follows either  
 271 a normal or uniform distribution, with same mean 0 and variance 1. The values for  $\pi_{\text{Sl}}$  and  $\pi_{\text{Cv}}$  translate well  
 272 the perceived “trendiness” (for large  $\pi_{\text{Sl}}$ ) or “curviness” (for large  $\pi_{\text{Cv}}$ ) of reaction norms, but they may also  
 273 strongly depend on the statistical distribution of the environmental variable  $\varepsilon$ , as shown especially in the third  
 274 example of [Figure 2](#). In this example, the difference arises because the assumed environmental distributions  
 275 have different kurtosis (the scaled fourth central moment, related to  $V(\varepsilon^2)$  in [Equation 15](#)). Because  $V(\varepsilon^2)$  is  
 276 larger for the Gaussian, this distribution leads to larger  $\pi_{\text{Cv}}$  than the uniform.

277 When it is not possible to assume that  $\varepsilon$  is normally distributed (because it is discrete, or experimentally  
 278 constrained) and a quadratic assumption is not a good fit to the reaction norm, it is always possible to use  
 279 a higher-order polynomial model to approximate the true reaction norm, in line with theoretical work by  
 280 de Jong ([1990](#)), Gavrillets & Scheiner ([1993b](#)), and de Jong ([1995](#)). In this case, we can conduct an alternative

---

<sup>30</sup>removed: on

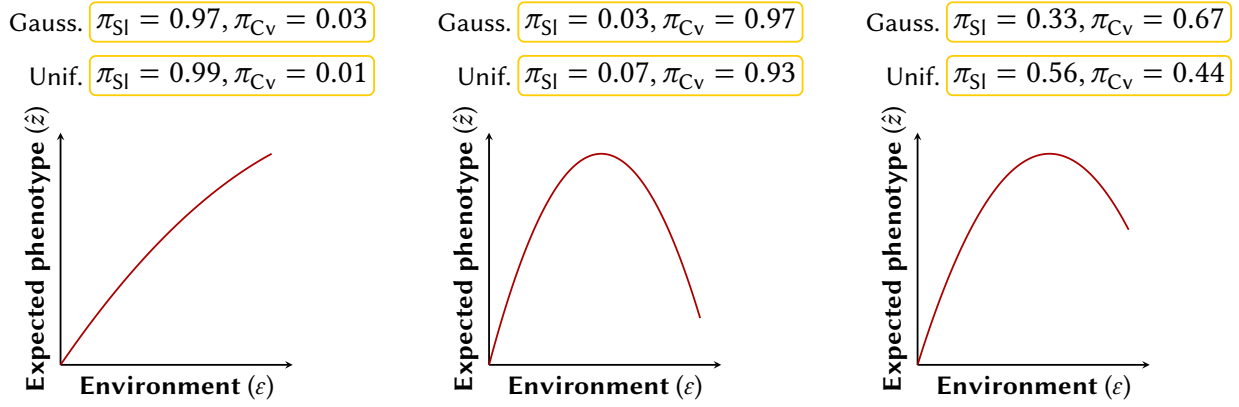


**Figure 2:** Computation of  $\pi_{Sl} = \pi_b$  and  $\pi_{Cv} = \pi_c$ , the relative contributions of linear and quadratic terms to phenotypic variation caused by the mean reaction norm, for different shapes of reaction norms, and two distributions of the environmental variable  $\epsilon$ : a standard Gaussian (of mean 0 and variance 1), and a uniform distribution between  $-\sqrt{3}$  and  $\sqrt{3}$  (of mean 0 and variance 1).

281 decomposition based on the parameters of the polynomial (rather than the mean slope and curvature of the  
 282 function), **using the fact that a polynomial curve is linear in its parameters**. To distinguish this parameter-  
 283 based decomposition from the specific decomposition in terms of slope and curvature, we use a different  
 284 notation. The relative contribution of a given exponent  $m$  in the polynomial to the variance caused by the  
 285 mean plasticity becomes (see [Appendix D2](#))

$$\varphi_m = \frac{\bar{\theta}_m^2 V(\epsilon^m)}{V_{\text{Plas}}}, \quad (16)$$

286 and the contribution of the covariance between exponents  $l$  and  $m$  is

$$\varphi_{lm} = \frac{2\bar{\theta}_l \bar{\theta}_m \text{Cov}(\epsilon^l, \epsilon^m)}{V_{\text{Plas}}}. \quad (17)$$

287 Note that even with a symmetrical and mean-centred environment, the covariance between higher-order  
 288 exponents will not be zero in general, contrary to  $\epsilon$  and  $\epsilon^2$  in the quadratic case. Using orthogonal polynomials  
 289 would solve this issue of covariances, but at the cost of a more complex interpretation of the coefficients.  
 290 More generally, this  $\varphi$ -decomposition only relies on the assumption that the reaction norm is linear on its  
 291 parameters, which includes polynomials as a particularly useful special case. We summarise the requirements  
 292 and applications for the  $\pi$ - and  $\varphi$ -decomposition depending on the context in [Figure 3](#).

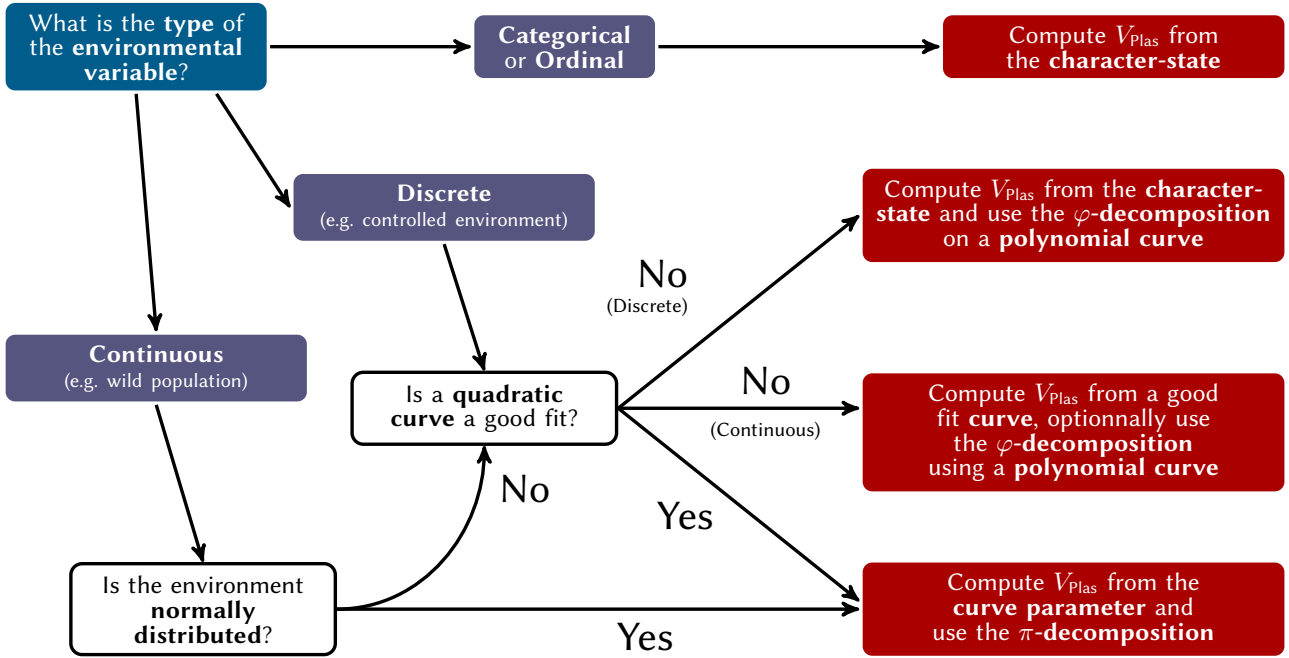


**Figure 3:** Decision tree summarising our suggested workflow for the computation and decomposition of  $V_{\text{Plas}}$ , depending on the nature of the environmental variable, its normality and the validity of a quadratic approximation of the reaction norm shape.

## Contributions of reaction norm parameters to the genetic variance

We can express the variance of the genotypic values of the reaction norms in Equation 5 in a slightly different, but more operational, manner:

$$V_{\text{Gen}} = V(\hat{z} - E_{g|\varepsilon}(\hat{z})) = E(V_{g|\varepsilon}(\hat{z})), \quad (18)$$

i.e. the total genotypic variance of the reaction norms is equal to the environment-specific genotypic variance averaged across environments. As explained above, this total genetic variance can be further decomposed into the genetic variance and the genotype-by-environment variance, i.e.  $V_{\text{Gen}} = V_G + V_{G \times E}$  (Falconer & Mackay 1996; Lynch & Walsh 1998; Des Marais et al. 2013). From an evolutionary perspective, the component of main interest is rather the total additive genetic variance of the reaction norm  $V_{\text{Add}}$ , which will be the main focus of this section. As a reminder, we here assume, that the experimental design allows for the inference of the additive genetic variance of the parameters of the reaction norm ( $G_z$  or  $G_\theta$  above), and that non-additive variance in the trait  $V_{\text{NonAdd}}$  only arises when the reaction norm is non-linear in the parameters (i.e. dominance and/or epistasis were not fitted in the statistical model). This assumption is for the sake of simplicity, as our framework can include such effects into  $V_{\text{Gen}}$  if needed.

A general way to relate the additive genetic variance of the trait to the additive genetic variances of the reaction norm parameters is through a vector that we describe as the reaction norm gradient, which we will

308 note  $\boldsymbol{\psi}_\varepsilon$  (following notations in de Villemereuil et al. 2016),

$$\boldsymbol{\psi}_\varepsilon = \mathbb{E}_g \left( \frac{\partial z}{\partial \boldsymbol{\theta}} \right)_\varepsilon, \quad (19)$$

309 where the subscript  $\varepsilon$  makes it clear that  $\boldsymbol{\psi}_\varepsilon$  will generally be a function of the environment. In the case of a  
 310 quadratic curve,  $\boldsymbol{\psi}_\varepsilon$  is the  $(1, \varepsilon, \varepsilon^2)^T$  vector (see Appendix C3 for a polynomial of arbitrary order). In the case  
 311 of a character-state model,  $\boldsymbol{\psi}_{\varepsilon_k}$  is a vector with 1 for the  $k$ th environmental level (or character state), and zero  
 312 elsewhere. Whether or not the reaction norm is linear in its parameters, the additive genetic variance of the  
 313 trait in a given environment  $\varepsilon$  is (Morrissey 2015; de Villemereuil et al. 2016, and see Appendix B),

$$V_{A|\varepsilon} = \boldsymbol{\psi}_\varepsilon^T \mathbf{G}_\theta \boldsymbol{\psi}_\varepsilon, \quad (20)$$

314 where superscript  $T$  denotes matrix transposition,  $\mathbf{G}_\theta$  the genetic covariance matrix of reaction norm pa-  
 315 rameters as defined in Equation 4 for the curve-parameter approach, and  $\mathbf{G}_\theta$  is  $\mathbf{G}_z$  from Equation 2 for the  
 316 character-state approach. The total additive genetic variance in the reaction norm,  $V_{\text{Add}}$ , is the average of  $V_{A|\varepsilon}$   
 317 across environments (see Appendix C1):

$$V_{\text{Add}} = \mathbb{E} \left( \boldsymbol{\psi}_\varepsilon^T \mathbf{G}_\theta \boldsymbol{\psi}_\varepsilon \right). \quad (21)$$

318 The [<sup>31</sup>]environment-blind additive genetic variance of the trait  $V_A$ , based on breeding values averaged  
 319 across environments, is (see Appendix C2)

$$V_A = \mathbb{E}(\boldsymbol{\psi}_\varepsilon)^T \mathbf{G}_\theta \mathbb{E}(\boldsymbol{\psi}_\varepsilon). \quad (22)$$

320 Although some elements of  $\mathbb{E}(\boldsymbol{\psi}_\varepsilon)$  and  $\mathbf{G}_\theta$  can be negative, the fact that  $\mathbf{G}_\theta$  is a variance-covariance matrix  
 321 ensures that  $V_A \geq 0$  (see Appendix C2). The additive genetic variance [<sup>32</sup>]arising from plasticity is thus (see  
 322 Appendix C2):

$$V_{A \times E} = V_{\text{Add}} - V_A = \mathbb{E} \left( \boldsymbol{\psi}_\varepsilon^T \mathbf{G}_\theta \boldsymbol{\psi}_\varepsilon \right) - \mathbb{E}(\boldsymbol{\psi}_\varepsilon)^T \mathbf{G}_\theta \mathbb{E}(\boldsymbol{\psi}_\varepsilon). \quad (23)$$

323 If we define  $\boldsymbol{\Psi} = \mathbb{E}(\boldsymbol{\psi}_\varepsilon \boldsymbol{\psi}_\varepsilon^T) - \mathbb{E}(\boldsymbol{\psi}_\varepsilon) \mathbb{E}(\boldsymbol{\psi}_\varepsilon)^T$ , the variance-covariance matrix of the reaction norm gradients  
 324 across environments, then a more intuitive way to express  $V_{A \times E}$  is as a sum, for all pairs of parameters, of the  
 325 (co)variance of their reaction norm gradient across environments (in  $\boldsymbol{\Psi}$ ) and their additive genetic (co)variance

---

<sup>31</sup>removed: marginal

<sup>32</sup>removed: in

326 (in  $G_\theta$ ):

$$V_{A \times E} = \sum_{i,j} \Psi_{(i,j)} G_{\theta(i,j)} = \text{Tr}(\Psi G_\theta), \quad (24)$$

327 where  $\text{Tr}$  is the trace of a matrix. All of the quantities above can be divided by  $V_P$  to get the corresponding  
328 heritabilities.

329 To illustrate with an example, for a quadratic reaction norm with mean-centred environment as shown  
330 in [Figure 1](#),  $\psi_\varepsilon = (1, \varepsilon, \varepsilon^2)$  and thus we have (see [Appendix C3](#))

$$\begin{aligned} V_{\text{Add}} &= V_a + (V_b + 2C_{ac})E(\varepsilon^2) + V_c E(\varepsilon^4), \\ V_A &= V_a + 2C_{ac}E(\varepsilon^2) + V_c E(\varepsilon^2)^2, \\ V_{A \times E} &= V_b V(\varepsilon) + V_c V(\varepsilon^2), \end{aligned} \quad (25)$$

331 where  $V_a$ ,  $V_b$  and  $V_c$  are the additive genetic variances in the parameters  $a_g$ ,  $b_g$  and  $c_g$ , and  $C_{ac}$  is the additive  
332 genetic covariance between the intercept  $a_g$  and the second-order effect  $c_g$ . Those expressions are reminiscent  
333 of classical results from the theory of evolution of plasticity (e.g. [de Jong 1990](#); [Gavrilets & Scheiner 1993b](#)),  
334 especially regarding the crucial role of  $C_{ac}$  in the evolution of quadratic reaction norms, but here distinguish-  
335 ing three important components of the additive genetic variance of reaction norms. In particular, we see how  
336 the additive genetic variance [[.33](#)] arising from plasticity,  $V_{A \times E}$ , can be simply expressed as the sum of the  
337 products of the variances in the reaction norm gradients (here the environment and its squared value) and the  
338 corresponding additive genetic variance in the parameters (here  $b_g$  and  $c_g$  in [Equation 12](#)). This means that,  
339 in the quadratic case, genetic variances in slope and curvature directly translate into variance [[.34](#)] arising  
340 from plasticity, as they should. By contrast,  $V_A$  does not solely depend on the variance in the intercept  $V_a$ , but  
341 also on the quadratic coefficient, more specifically its covariance with the intercept.

342 The expressions for these variance components in the character-state approach are best described directly  
343 from the  $G_z$  matrix. The total additive genetic variance along the reaction norm,  $V_{\text{Add}}$ , is the average of the  
344 additive genetic variance in each environment, i.e. the average of the diagonal elements of the  $G_z$ . The [[.35](#)]  
345 ]environment-blind additive genetic variance of the trait,  $V_A$ , is the average of all the elements of the  $G_z$   
346 matrix. Finally, the variance  $V_{A \times E}$  is the sum of the products of the (co)variances in the frequency of each  
347 environment and the additive genetic (co)variances in  $G_z$ . We illustrate in [Appendix C4](#) the relationship  
348 between the structure in the  $G_z$  matrix and the additive genetic variances, but a simplified statement is that  
349  $V_{A \times E} > 0$  as soon as the correlation between environments are different from 1 and/or variances in the  
350 diagonal are not all equal.

351 To further decompose genetic variation in the reaction norms, we first note that here, the reaction norm

---

<sup>33</sup>removed: in

<sup>34</sup>removed: in

<sup>35</sup>removed: marginal



352 parameters are the focus of the decomposition, rather than shape characteristics like the slope or curvature  
 353 (with the exception of a quadratic reaction norm, the only case were they are formally linked). Because  
 354 Equation 21 is a sum of products, and since  $G_\theta$  is a constant, we can isolate each term of the resulting sum as:

$$\gamma_i = \frac{E_\varepsilon(\psi_{\varepsilon,i}^2) V_g(\theta_i)}{V_{\text{Add}}}, \quad \gamma_{ij} = \frac{2E_\varepsilon(\psi_{\varepsilon,i}\psi_{\varepsilon,j}) \text{Cov}_g(\theta_i, \theta_j)}{V_{\text{Add}}}, \quad \sum_i \gamma_i + \sum_{i<j} \gamma_{ij} = 1. \quad (26)$$

355 Here,  $\gamma_i$  provides the contribution of the  $i$ th parameter in the model to the total additive genetic variance  
 356  $V_{\text{Add}}$ , while  $\gamma_{ij}$  provides the contribution of the covariation between parameters  $i$  and  $j$  to  $V_{\text{Add}}$ . As such,  
 357 this “ $\gamma$ -decomposition” (where gamma refers to g for Genetics) measures the relative importance of genetic  
 358 variances and covariances of the parameters to the evolvability of the plastic trait. Large values of  $\gamma_i$  indicate  
 359 that genetic variation in the  $i$ th parameter translate into a large proportion of the genetic variation in the trait.  
 360 Also, large positive or negative values for  $[\dots^{36}] \gamma_{ij}$  indicate that covariation between parameters  $i$  and  $j$  can  
 361 have a large impact in increasing or reducing genetic variation in the trait.

362 It is also possible to focus on the additive genetic variation  $[\dots^{37}]$  arising from plasticity,  $V_{\text{A}\times\text{E}}$ ,  $[\dots^{38}]$  which  
 363 yields:

$$l_i = \frac{V(\psi_{\varepsilon,i}) V_g(\theta_i)}{V_{\text{A}\times\text{E}}}, \quad l_{ij} = \frac{2\text{Cov}_\varepsilon(\psi_{\varepsilon,i}, \psi_{\varepsilon,j}) \text{Cov}_g(\theta_i, \theta_j)}{V_{\text{A}\times\text{E}}}, \quad \sum_i l_i + \sum_{i<j} l_{ij} = 1. \quad (27)$$

364 This “ $l$ -decomposition” (where iota refers to i for Interaction) highlights the fact that  $V_{\text{A}\times\text{E}}$  is the sum of the  
 365 products of (co)variances in elements of the reaction norm gradient  $\psi_\varepsilon$  and the additive genetic (co)variances  
 366 in the parameters.

367 For a quadratic reaction norm as in Equation 12 with a mean-centred environment, this yields:

$$\gamma_a = \frac{V_a}{V_{\text{Add}}}, \quad \gamma_b = \frac{V_b E(\varepsilon^2)}{V_{\text{Add}}}, \quad \gamma_c = \frac{V_c E(\varepsilon^2)^2}{V_{\text{Add}}}, \quad \gamma_{ac} = \frac{2C_{ac} E(\varepsilon^2)}{V_{\text{Add}}}, \quad l_b = \frac{V_b V(\varepsilon)}{V_{\text{A}\times\text{E}}}, \quad l_c = \frac{V_c V(\varepsilon^2)}{V_{\text{A}\times\text{E}}}. \quad (28)$$

368 Note that since the environment has been mean-centred, we have  $V(\varepsilon) = E(\varepsilon^2)$  since  $E(\varepsilon)^2 = 0$ , and thus  
 369  $\gamma_b = l_b$ , i.e. in the quadratic case, all of the genetic variation in the slope contributes to the genetic variance  
 370  $[\dots^{39}]$  arising from plasticity. Note also that genetic variance in reaction norm intercept  $a$  does not contribute  
 371 to the heritability  $[\dots^{40}]$  from plasticity ( $l_a = 0$ ).

372 For the character-state approach, such decomposition  $[\dots^{41}]$  would be less informative about the potential

<sup>36</sup>removed:  $\gamma_{ij}$

<sup>37</sup>removed: in

<sup>38</sup>removed: rather than the reaction norm itself,

<sup>39</sup>removed: in

<sup>40</sup>removed: of

<sup>41</sup>removed: can be performed but yields as many parameters as there are environments for  $\gamma$ , and pairwise combinations of environments for  $l$ . They directly depend on the additive genetic variance in each environment, weighed by its frequency in the experimental setting for  $\gamma$ ; and on the product between the (co)variance in frequency of the environment and the additive genetic (co)variance in or between environments for  $l$ . While these quantities can be informative about particular (couple of) environment (e.g. large  $\gamma_k$  would sign that the  $k$ th environment is associated with a large genetic variance, compared to the others), they are

373 for (and [..<sup>42</sup> ][..<sup>43</sup> ]constraints on) reaction norm evolution. Instead, we can define [..<sup>44</sup> ]an effective number  
374 of character states (as proposed for general multivariate phenotypes by Kirkpatrick 2009) as

$$n_e = \sum_i \frac{\lambda_i}{\lambda_1}, \quad (29)$$

375 where  $\lambda_i$  is the  $i^{\text{th}}$  eigenvalue of  $G_z$  ranked by size (i.e.,  $\lambda_1$  is the largest eigenvalue). [..<sup>45</sup> ]Strong genetic  
376 correlations of phenotypes across environments lead to small  $n_e$ [..<sup>46</sup> ], whereby reaction norm evolution is  
377 highly constrained [..<sup>47</sup> ](with the limit of  $n_e = 1$  corresponding to the strongest constraint). Conversely,  
378 weak genetic correlations across environments leave more degrees of freedom for reaction norms to evolve,  
379 causing a large  $n_e$ [..<sup>48</sup> ], close to the actual number of assayed environments. This  $n_e$  metric does not capture  
380 all aspects of reaction norm evolvability, and is best combined with the ratio  $V_{A \times E}/V_{\text{Add}}$  [..<sup>49</sup> ]of the proportion  
381 of total genetic variance [..<sup>50</sup> ]due to genetic variance in plasticity[..<sup>51</sup> ]. Unfortunately,  $n_e$  is estimated with  
382 a strong bias due to the overestimation of the leading eigenvalue of  $G_z$  (Lawley 1956), making it less useful  
383 in practice than in theory. We thus do not develop this metric further.

## 384 Parameter estimation and variance partitioning in practice

### 385 Estimating the parameters

386 All the parameters mentioned in the previous section can be estimated through commonly used statistical  
387 frameworks. For the character-state approach (Equation 2), a [..<sup>52</sup> ]random-parameter model can be used,  
388 or alternatively a “multi-trait” model (Rovelli et al. 2020; Mitchell & Houslay 2021). We will focus here on  
389 the former, which is more easily implemented while seemingly scarcely used in the literature on plasticity.

---

certainly not summary quantities of the  $G_z$  matrix and are difficult to easily relate to evolvability and constraints on reaction norms shape. The variances  $V_{\text{Add}}$ ,  $V_A$

<sup>42</sup>removed:  $V_{A \times E}$  are more interesting summary statistics in this particular context. Another interesting summary quantity can be provided by the toolbox of multivariate quantitative genetics. Following

<sup>43</sup>removed: ,

<sup>44</sup>removed: the

<sup>45</sup>removed: Large

<sup>46</sup>removed: close to the actual number of assayed environments means that genetic variance is well balanced and little correlated across environments . Conversely,  $n_e$  near 1 means that most genetic variation lies along a single combination of character states, such that

<sup>47</sup>removed: , i.e. the genetic correlations are very high between the environments. However, it would be wrong to equate  $n_e = 1$  with an absence of genetic variance in plasticity: if the genetic variances within environments (i.e. the diagonal elements of  $G_z$ ) are variable while  $n_e = 1$ , this results in more evolvability in some environments, thus  $V_{A \times E} > 0$ . Reciprocally, a maximal value for

<sup>48</sup>removed: (i.e. equal to the number of environments) does not mean that the genetic variance in plasticity is maximised at the expense of additive genetic variance in the trait: for example, when there is no genetic covariances between environments and equal genetic variances within environments,  $n_e$  is maximised, but  $V_A$  is not zero. As a result, a combined interpretation of

<sup>49</sup>removed: (i.e. how much of the

<sup>50</sup>removed: in the reaction norm consists of

<sup>51</sup>removed: generates an interesting summary of the main properties of the  $G_z$  matrix in the context of a character-state.

<sup>52</sup>removed: random-intercept

390 In [..<sup>53</sup> ]the **random-parameter** model, the environment is considered as a categorical variable, to which a  
391 random effect is added using the genotype as the grouping factor. In the curve-parameter approach, the  
392 appropriate models will be [..<sup>54</sup> ]**random-parameter** models for a polynomial approach (as mentioned in  
393 Morrissey & Liefting 2016), or non-linear mixed models, fitting the reaction norm function  $f(\varepsilon, \theta)$  to the  
394 data. [..<sup>55</sup> ]**Genotype-specific parameters, such as** the intercept, slope, and any higher-order effects [..<sup>56</sup> ]**of a**  
395 **polynomial function[..<sup>57</sup> ], are treated as random'**

396 Since the parameters are estimated with noise, it is important to account for the impact of estimation  
397 uncertainty when computing variance components. In particular, while variances directly obtained using  
398 random effects (e.g. genetic variances) are expected to be unbiased, the variances arising from fixed effects  
399 (e.g. variances related to  $V_{\text{Plas}}$ ) should be corrected for biases due to uncertainty (as the adjusted  $R^2$  does for  
400 example). Details are provided in [Appendix E](#).

401 To compute the total phenotypic variance required to get the estimates  $\hat{P}_{\text{RN}}^2$ ,  $\hat{H}_{\text{RN}}^2$  and  $\hat{h}_{\text{RN}}^2$ , we advise using  
402 the sum of all estimated components rather the raw sample variance. The former is common practice in most  
403 quantitative genetics inference to account for potential imbalance in the experimental or sampling design  
404 (Wilson et al. 2010; de Villemereuil et al. 2018).

405 We provide an R package, named Reacnorm [github.com/devillemereuil/Reacnorm](https://github.com/devillemereuil/Reacnorm), providing functions  
406 implementing the variance decomposition based on raw outputs of statistical models. A tutorial is shipped  
407 with the package, as an R vignette, showing how to implement such models using the Bayesian brms R pack-  
408 ages (Bürkner 2017), along with Reacnorm.

## 409 **Perfect modelling of quadratic curves**

410 We simulated phenotypic data conforming to a quadratic reaction norm, to evaluate the performance of the  
411 proposed approach when the reaction norm truly is quadratic. We considered both a discrete and continu-  
412 ous environment. For the discrete environment, we considered  $N_{\text{Gen}} = 20$  or 5 different genotypes and an  
413 environmental gradient of  $N_{\text{Env}} = 10$  or 4 values, equally spaced from -2 to 2. We sampled  $N_{\text{Rep}} = N_{\text{Gen}}$   
414 individual measures for each genotype [..<sup>58</sup> ]**within an environment**. For the continuous environment, we  
415 drew  $N_{\text{Env}} = 10$  or 4 values from a normal distribution for each of the  $N_{\text{Gen}} = 200$  or 50 genotypes[..<sup>59</sup>  
416 ], **without repeats contrary to the discrete case. In both cases, a residual** noise was applied around each  
417 measure [..<sup>60</sup> ]with a residual variance  $V_{\text{Res}} = 0.25$ . In all cases, we defined a quadratic curve with average

---

<sup>53</sup>removed: a random-intercept

<sup>54</sup>removed: random-slope

<sup>55</sup>removed: Random effects are fitted to the parameters of this function (with the genotype as grouping factor), e.g.

<sup>56</sup>removed: for

<sup>57</sup>removed: .

<sup>58</sup>removed: with a residual variance  $V_{\text{Res}} = 0.25$

<sup>59</sup>removed: . Residual

<sup>60</sup>removed: for each genotype

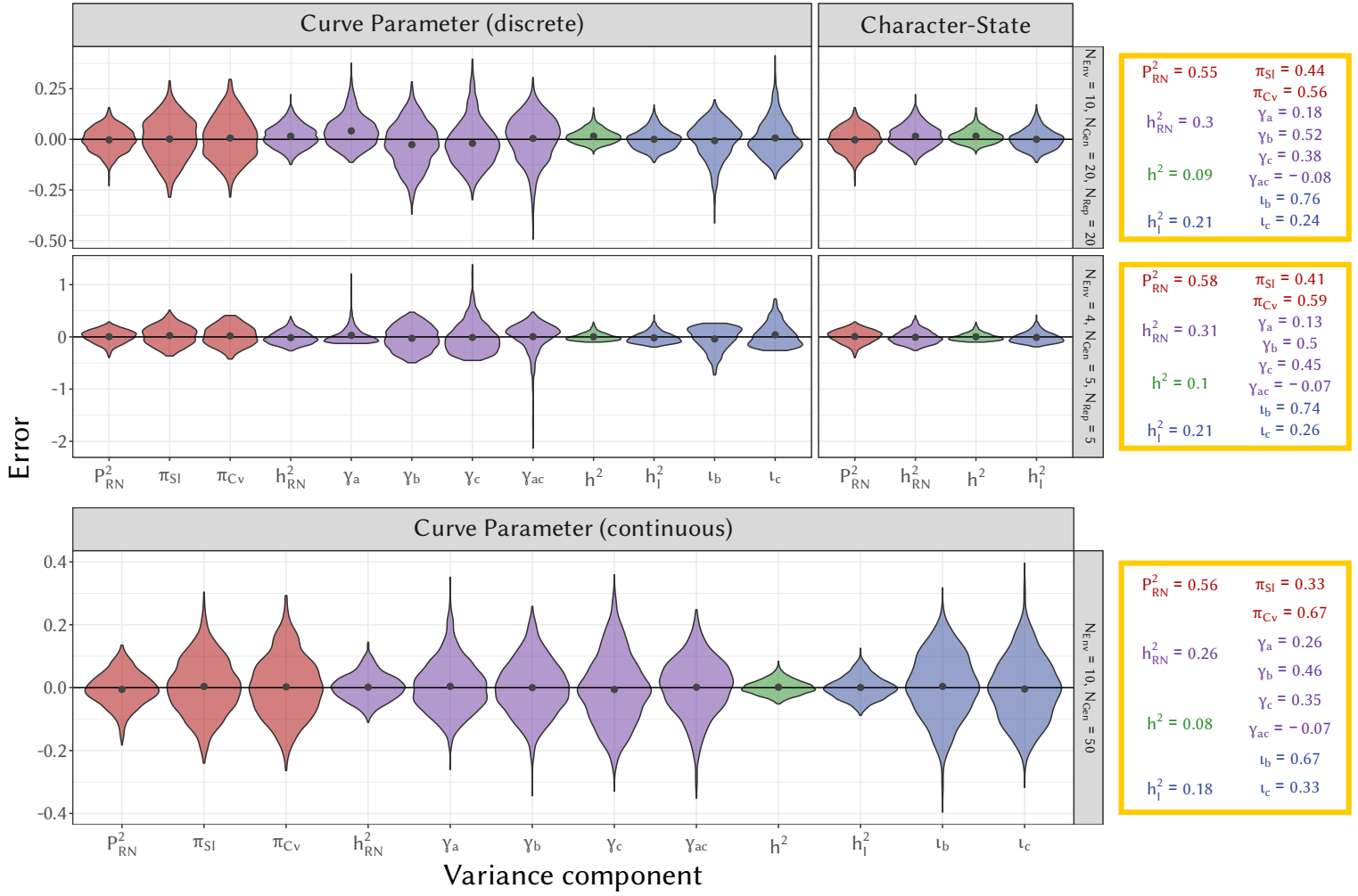


**Figure 4:** Distribution of the error (difference between the inferred and true value) for each the inferred variance components for three scenarios: two discrete ( $N_{env}$ : number of environments,  $N_{Gen}$ : number of different genotypes,  $N_{Rep}$ : number of replicates per genotype) and one continuous ( $N_{env}$ : number of environment tested per genotype,  $N_{Gen}$ : number of different genotypes). The grey dots correspond to the average over the 1000 simulations. The character-state approach was impossible for the continuous environment scenario. The yellow boxes on the right show the estimates for  $\hat{P}_{RN}^2$  (proportion of variance generated by the plasticity in the mean reaction norm),  $\hat{h}_{RN}^2$  (total heritability of the reaction norm),  $\hat{h}^2$  (environment-blind heritability<sup>[.a]</sup>) and  $\hat{h}_1^2$  (heritability<sup>[.b]</sup> from plasticity) for both the curve-parameter and character-state approaches. For the curve-parameter, the  $\pi$ -decomposition of  $\hat{P}_{RN}^2$  into  $\pi_{SI}$  (contribution of the slope) and  $\pi_{Cv}$  (contribution of the curvature); the  $\gamma$ -decomposition of  $\hat{h}_{RN}^2$  into  $\gamma_a$  (genetic contribution of the intercept),  $\gamma_b$  (genetic contribution of the slope),  $\gamma_c$  (genetic contribution of the curvature) and  $\gamma_{ac}$  (genetic contribution of the covariance between the intercept and the curvature) and the  $l$ -decomposition of  $\hat{h}_1^2$  into  $l_b$  (slope) and  $l_c$  (curvature) are also shown.<sup>[.c]</sup>

<sup>a</sup>removed: based on average breeding values

<sup>b</sup>removed: of

<sup>c</sup>removed: The effective number of dimensions  $n_e$  from the character-state is not shown, due to an important bias impacting the comparison with the other parameters.

418 parameters  $\bar{\theta} = (1.5, 0.5, -0.5)$  for intercept, slope and curvature. We then drew  $N_{Gen}$  different genotype-

419 specific vectors of curve-parameter  $\theta$  from a multivariate normal distribution with mean  $\bar{\theta}$  and (genotypic)

420 variance-covariance matrix

$$G_{\theta} = \begin{pmatrix} 0.090 & -0.024 & -0.012 \\ -0.024 & 0.160 & 0.008 \\ -0.012 & 0.008 & 0.040 \end{pmatrix}.$$

421 **Figure 1** displays examples of curves resulting from these parameters. The simulation process was repeated  
422 1000 times for each scenario, and for each simulated dataset, we ran estimations using the lme4 R package  
423 (Bates et al. 2015) under the curve-parameter (for discrete and continuous environment) and character-state  
424 (only for discrete environment) approaches, in order to check how these approaches compare in practice.

425 From the curve-parameter models, we computed  $\hat{V}_{\text{Plas}}$  (accounting for the uncertainty in fixed effects),  
426 then  $\hat{P}_{\text{RN}}^2$ . We also computed the  $\pi$ -decomposition ( $\hat{\pi}_{\text{SI}}$  and  $\hat{\pi}_{\text{CV}}$ , Equation 14), since the true reaction norm  
427 is quadratic here, as well as  $\hat{h}_{\text{RN}}^2$ ,  $\hat{h}^2$  and  $\hat{h}_1^2$  as in Equation 9. We then applied the  $\gamma$ -decomposition to  $\hat{h}_{\text{RN}}^2$   
428 (Equation 26):  $\hat{\gamma}_a$  (impact of the genetic variation of the intercept),  $\hat{\gamma}_b$  (for the slope),  $\hat{\gamma}_c$  (for of the curvature)  
429 and  $\hat{\gamma}_{ac}$  (for the covariance between the intercept and curvature). Similarly, we applied the  $\iota$ -decomposition  
430 to  $\hat{h}_1^2$  (Equation 27):  $\iota_b$  (for the slope) and  $\iota_c$  (for the curvature). From the character-state model, we computed  
431 only  $\hat{P}_{\text{RN}}^2$ ,  $\hat{h}_{\text{RN}}^2$ ,  $\hat{h}^2$  and  $\hat{h}_1^2$ .

432 The yellow boxes in **Figure 4** display the theoretical expected values for the different parameters for three  
433 scenarios of environmental variation (two discrete, one continuous; other scenarios are shown in Appendix F).  
434 Using the first discrete scenario as a reference for now, most of the total phenotypic variance comes from the  
435 average plasticity ( $P_{\text{RN}}^2 = 0.55$ ). This, in turns, includes a large contribution from the curvature ( $\pi_{\text{CV}} = 0.56$ )  
436 of the average reaction norm, more than from its slope ( $\pi_{\text{SI}} = 0.44$ ). The total heritability of the reaction  
437 norm is substantial ( $h_{\text{RN}}^2 = 0.3$ ), but interestingly most of it is due to the heritability [<sup>61</sup>]from plasticity  
438 ( $h_1^2 = 0.21$ ), while the [<sup>62</sup>]environment-blind heritability of the trait is only  $h^2 = 0.08$ . Contrary to the  
439 average shape, most of the additive genetic variation comes from the slope, both when considering the total  
440 reaction norm ( $\gamma_b = 0.52$ ), or plasticity alone ( $\iota_b = 0.76$ ). All scenarios share the same underlying parameters  
441  $\theta$  and  $G_{\theta}$ , resulting in very comparable values for our variance decomposition (i.e.  $P_{\text{RN}}^2$  and the heritabilities)  
442 across the different environmental sampling scheme. By contrast, the environmental sampling scheme (es-  
443 pecially discrete v. continuous distribution) can substantially impact the expected values of the  $\pi$ -,  $\gamma$ - and  
444  $\iota$ -decompositions. This is especially true when switching from the discrete to the continuous scenarios (e.g.  
445  $\pi_{\text{SI}} = 0.44$  for the first discrete scenario while  $\pi_{\text{SI}} = 0.33$  for the continuous scenario). [<sup>63</sup>]

446 Switching to the error in the estimation of the parameters (left panels of **Figure 4**), we see first that both the

---

<sup>61</sup>removed: of plasticity ( $h_{\text{RN}}^2 = 0.21$ )

<sup>62</sup>removed: marginal

<sup>63</sup>removed: Interestingly, the theoretical effective number of environment  $n_e$  is very stable when comparing the first (4 environ-  
ments) and second (10 environments) discrete scenarios ( $n_e = 2$  v.  $n_e = 1.9$ ), which is due to the constraining shape of the quadratic  
reaction norm.

447 character-state and curve-parameter approaches allow for unbiased inference (Wilcoxon’s rank test,  $p > 0.05$ ),  
448 apart from a slight bias in the heritabilities ( $\hat{h}_{RN}^2$ ,  $\hat{h}^2$  and  $\hat{h}_1^2$ ) and some of their  $\gamma$  and  $\iota$  components in the discrete  
449 scenarios ( $< 5\%$  relative bias, Wilcoxon’s rank test,  $p < 0.05$ ), notably due to a slight overestimation of the  
450 genetic variance of the intercept (visible in the top row of Figure 4). [..<sup>64</sup> ] [..<sup>65</sup> ] [..<sup>66</sup> ] For the discrete case,  
451 the precision of the estimates was not much influenced by the number of environments and depended more  
452 on the number of genotypes (see Figure S1). For the continuous case, both the number of environments and  
453 genotypes influenced the precision of estimates (see Figure S2). As a sanity check, we also verified that  $\hat{V}_{Tot}$   
454 (not shown in Figure 4) reflected the raw phenotypic variance with extreme precision (correlation  $> 99\%$ )  
455 in the discrete case and very good precision (correlation  $> 87\%$ ) in the continuous case. The difference  
456 between these two types of scenarios is explained by how the stochasticity in environmental values differs  
457 among them. Importantly, the results in Figure 4) also illustrate the exact equivalence, in the discrete case,  
458 between the curve-parameter and character-state approaches, as the distributions of  $\hat{P}_{RN}^2$  and  $\hat{h}_{RN}^2$  were nearly  
459 identical (Figure 4, correlation  $> 99\%$ ) between the two approaches. This means that our variance partitioning  
460 is not impacted by which approach is chosen to study plasticity, as long as the curve-parameter approach  
461 captures the true reaction norm shape. When this does not hold, the differences between estimates from  
462 these alternative approaches can be exploited efficiently, as we describe below.

## 463 Imperfect modelling of a non-polynomial reaction norm

464 The true shapes of reaction norms are generally unknown and may be complex, such that any curve-parameter  
465 model is likely to be mis-specified to some extent. In the case of a discrete environment, the character-state  
466 approach is arguably more general, as it does not assume anything about the “true” shape of the reaction  
467 norm (as pointed out previously by de Jong 1995). Nonetheless, having access to curve-parameters is often  
468 very interesting and more actionable (even in cases where the linear and quadratic components cannot be  
469 interpreted as the average slope and curvature), especially to predict evolution of phenotypic plasticity (see  
470 also de Jong 1995). To get the best of both worlds, we rely on the ability of the character-state approach  
471 to recover  $P_{RN}^2$ , using it as an “anchor”, to assess the performance of a given curve. Note that, under these  
472 circumstances, it is not possible to obtain the most natural  $\pi$ -decomposition in Equation 14, so we instead rely  
473 on the  $\varphi$ -decomposition in Equation 16 (here taken at the second order). Because of this, we need to assess  
474 how “bad” our simplification using an imperfect curve is. To do so, we compute the ratio of the variance

<sup>64</sup>removed: A notable exception, not shown in the graphics of

<sup>65</sup>removed: , was the effective number of dimensions,  $n_e$ , for the character-state. The relative bias was between  $-12\%$  and  $-35\%$  (Wilcoxon’s rank test,  $p < 0.05$ ), and was mainly explained by an overestimation of the dominant eigenvalue  $\lambda_1$  in

<sup>66</sup>removed: .

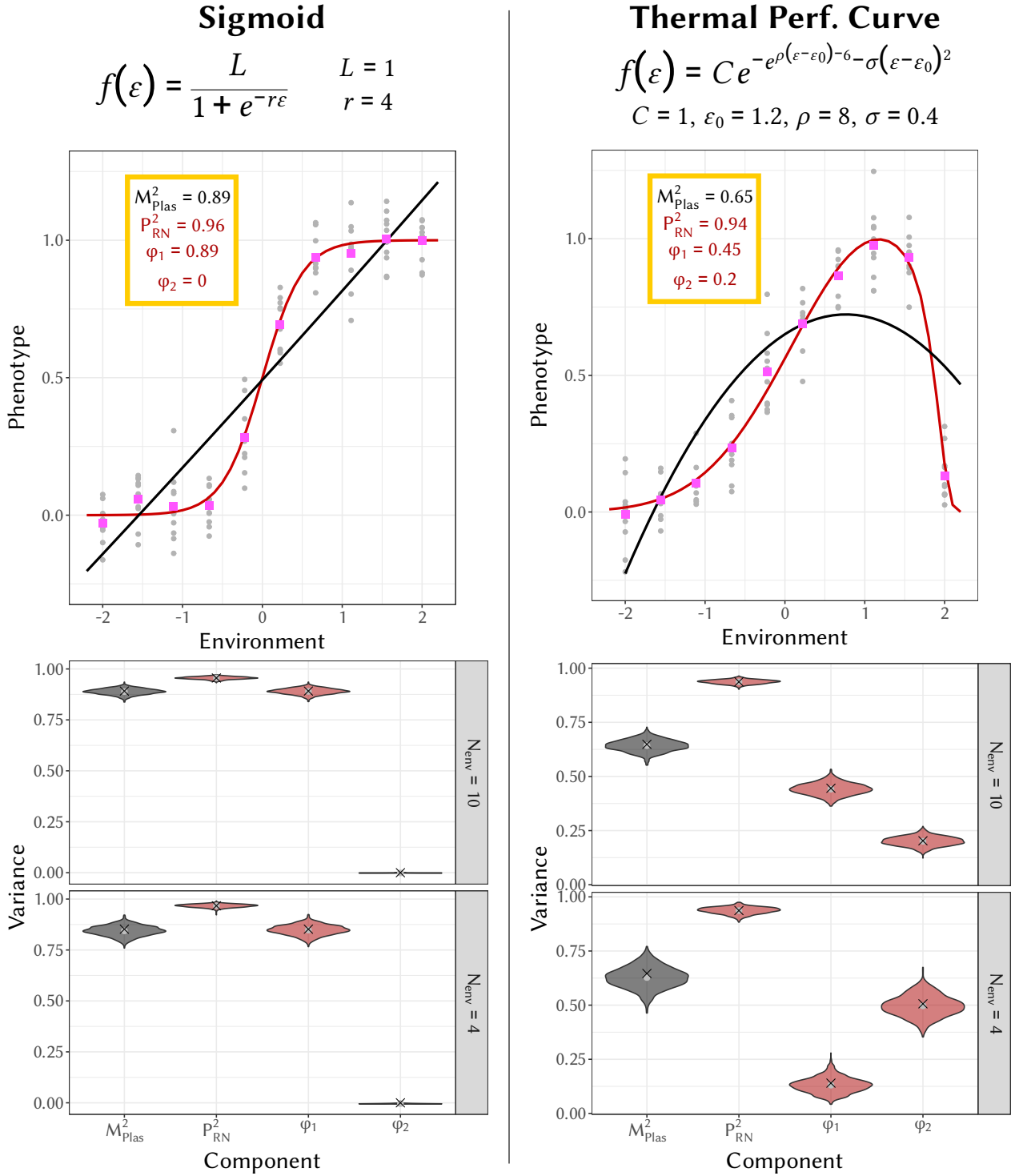


**Figure 5:** Estimation of the variance of the reaction norm when the true shape (sigmoid on the left, Gompertz-Gaussian performance curve on the right, red lines on top graphs) is unknown and approximated from a polynomial function. The estimated reaction norms using a polynomial function (black line, top graphs) only account for a part of the reaction norm shape, while the ANOVA estimation (pink dots, top graphs) fit the true shape more accurately. As a result, the model is expected to explain only a part  $M_{\text{Plas}}^2$  of phenotypic variance due to plasticity. On the bottom rows, the error distribution are shown for  $M_{\text{Plas}}^2$ ,  $P_{\text{Plas}}^2$ ,  $\varphi_1$  and  $\varphi_2$  (grey dots are the average estimated values, black crosses are the expected true values).

475 modelled by the polynomial curve to the total variance due to phenotypic plasticity:

$$M_{\text{Plas}}^2 = \frac{\hat{V}_{\text{mod}}}{\hat{V}_{\text{Plas}}} [\dots] \quad (30)$$

476 where both  $\hat{V}_{\text{mod}}$  and  $\hat{V}_{\text{Plas}}$  are bias-corrected. It is important to note here that  $M_{\text{Plas}}^2$  is just a convenient way  
477 to quantify the amount of  $\hat{V}_{\text{Plas}}$  explained by the chosen parametric curve, and should not be used to perform  
478 model selection. Model selection is a complex matter and we refer the readers to published reviews on this  
479 subject (e.g. Johnson & Omland 2004; Tredennick et al. 2021).

480 In order to demonstrate the soundness and usefulness of this approach, we simulated datasets following  
481 relatively common curves that are not well-captured by a second order polynomial: a logistic sigmoid (here-  
482 after sigmoid scenario), or a Gompertz-Gaussian thermal performance curve (hereafter TPC scenario, see  
483 Figure 5). We assumed that the environment is sampled at either 10 or 4 values. For each of these conditions,  
484 we simulated 1000 datasets, with 10 measures *per* environment (for the sake of simplicity, and given the focus  
485 on  $\hat{P}_{\text{RN}}^2$  here, we did not include different genotypes in these simulations). We estimated the parameters of a  
486 polynomial model, and computed the relative contributions of the first- and second-order parameters using  
487 Equation 16. In addition, we computed the unbiased estimates of the variance explained by our polynomial  
488 or character-state models to obtain  $M_{\text{Plas}}^2$ .

489 Our results show that, as expected, the polynomial function is an imperfect proxy of our complex shapes  
490 (Figure 5,  $M_{\text{Plas}}^2 = 0.89$  for the sigmoid and  $M_{\text{Plas}}^2 = 0.65$  for the TPC), but using the character-state approach  
491 allows retrieving the total plastic variance without bias. The approach described here is thus useful to compare  
492 a given reaction norm model (e.g. a polynomial function) to an unknown true shape of the reaction norm,  
493 in a case where environment is discretised. In more detail, the linear component was the most important  
494 component to explain the phenotypic variation for the sigmoid scenario ( $\varphi_1 = 0.89$ , same as the total model).  
495 This was because the quadratic component was always estimated close to zero ( $< 10^{-3}$ ), thus no variance  
496 was explained by the quadratic component ( $\varphi_2 = 0$ ). Of course, the sigmoid is not a straight line either, and  
497 some remaining variance unexplained by the polynomial curve ( $1 - 0.89 = 0.11$ ) could have been explained  
498 by higher-order effects (e.g. cubic effect and higher). By contrast, for the TPC scenario, while the linear  
499 component was an important factor ( $\varphi_1 = 0.47$ ), the quadratic component also explained quite a lot of the  
500 variance as well ( $\varphi_2 = 0.2$ ). Again, higher-order effect, including at least a cubic effect, would have explained  
501 more of the variance arising from the average shape of plasticity.

502 This example illustrates the usefulness of a combined curve-parameter and character-state approach to  
503 study the shape of reaction norms of a discretely sampled environment. While the character-state approach  
504 provides a widely applicable estimation of  $\hat{P}_{\text{RN}}^2$  (if the environment is discretised), the curve-parameter ap-  
505 proach provides interpretable information about (at least) first- and second-order parameters of the reaction  
506 norm (although they might depart more or less strongly from its average slope and curvature), which helps  
507 describing where most phenotypic variance lies. Our ratio  $M_{\text{Plas}}^2$  can then be used to evaluate how well a  
508 chosen polynomial function models an actual reaction norm.



## 509 Estimation of non-linear models

510 Although we have focused so far on models that are linear in its parameters, the main strength of our approach  
511 is its generality: it can be applied to any arbitrary functions (provided it is differentiable). This requires  
512 numerically computing integrals for  $V_{\text{Plas}}$  (for  $\hat{P}_{\text{RN}}^2$ ),  $\pi_{\text{Sl}}$ ,  $\pi_{\text{Cv}}$  and  $\boldsymbol{\psi}_\epsilon$  (for the heritabilities), but this can be solved  
513 with efficient algorithms. We illustrate this by introducing genetic variation in the parameters of the sigmoid  
514 and TPC reaction norms illustrated in Figure 5 (top panels). We used a non-zero, but small, residual variance  
515 ( $V_{\text{R}} = 0.0001$ ) to avoid numerical issues typical when running thousands of non-linear models. We focused  
516 on a continuous environment, and estimated the actual functions used to generate the datasets, using the non-  
517 linear modelling function of nlme package (Pinheiro et al. 2009). We used the cubature package (Narasimhan  
518 et al. 2023), as in the QGglmm package (de Villemereuil et al. 2016), to compute parameters linked to the  
519 variance decomposition, and, further, the  $\pi$ -,  $\gamma$ - and  $\iota$ -decomposition. We simulated 1000 datasets for each  
520 scenario, consisting of 200 genotypes measured each in 10 different environments, randomly sampled from a  
521 normal distribution.

522 We retrieved our simulated parameters without bias using the nlme function, except for a slight bias  
523 (Wilcoxon's rank test,  $p < 0.05$ ) in the variance of  $r$  (latent slope) in the sigmoid model and in  $C$  (height  
524 of the peak) in the TPC model. This translated into significant (Wilcoxon's rank test,  $p < 0.05$ ), but very  
525 limited bias (relative bias  $< 5\%$ ) in our derived parameters (Figure 6, bottom panels). Moreover, the sum of  
526 variance components ( $\hat{V}_{\text{Tot}}$ ) successfully reflects the total phenotypic variance, with a correlation between the  
527 two quantities  $> 91\%$ .

528 First focusing on the average shape of the reaction norm (Figure 6, top panel), one unfortunate aspect  
529 of running a non-linear model is that our bias correction described in Appendix E can no longer be applied.  
530 However, this bias is generally small provided the standard error is small for most parameters, and the result-  
531 ing bias in  $\hat{P}_{\text{RN}}^2$  is extremely small, and even non-significant for the sigmoid model. **This could of course be**  
532 **partly explained by a favourable context here, especially since the residual variance is relatively small.** An  
533 important distinction here is the difference between the curve defined by the average parameters  $f(\epsilon, \bar{\boldsymbol{\theta}})$  (Fig-  
534 ure 6, top panel, black curve) and the one defined by the local average phenotype  $E_{g|\epsilon}(\hat{z})$  (Figure 6, top panel,  
535 red curve), recalling that  $\hat{P}_{\text{RN}}^2$  is linked to the latter. While the two are very close for the sigmoid case, **[.**<sup>68</sup>  
536 **]they** differ quite visibly for the TPC one, due to a more pronounced non-linearity in the parameters in the  
537 latter. The average slope contributed the most to the overall plastic variance of the mean reaction norm for  
538 the sigmoid shape ( $\pi_{\text{Sl}} = 0.88$ ), with no impact of average curvature ( $\pi_{\text{Cv}} = 0$ ), close to the  $\varphi$ -decomposition in  
539 Figure 5. For the TPC scenario, the contribution of the average slope ( $\pi_{\text{Sl}} = 0.31$ ) and curvature ( $\pi_{\text{Cv}} = 0.35$ )  
540 are similar. In this case, the values are very different from the  $\varphi$ -decomposition in Figure 5 (although note

---

<sup>68</sup>removed: their

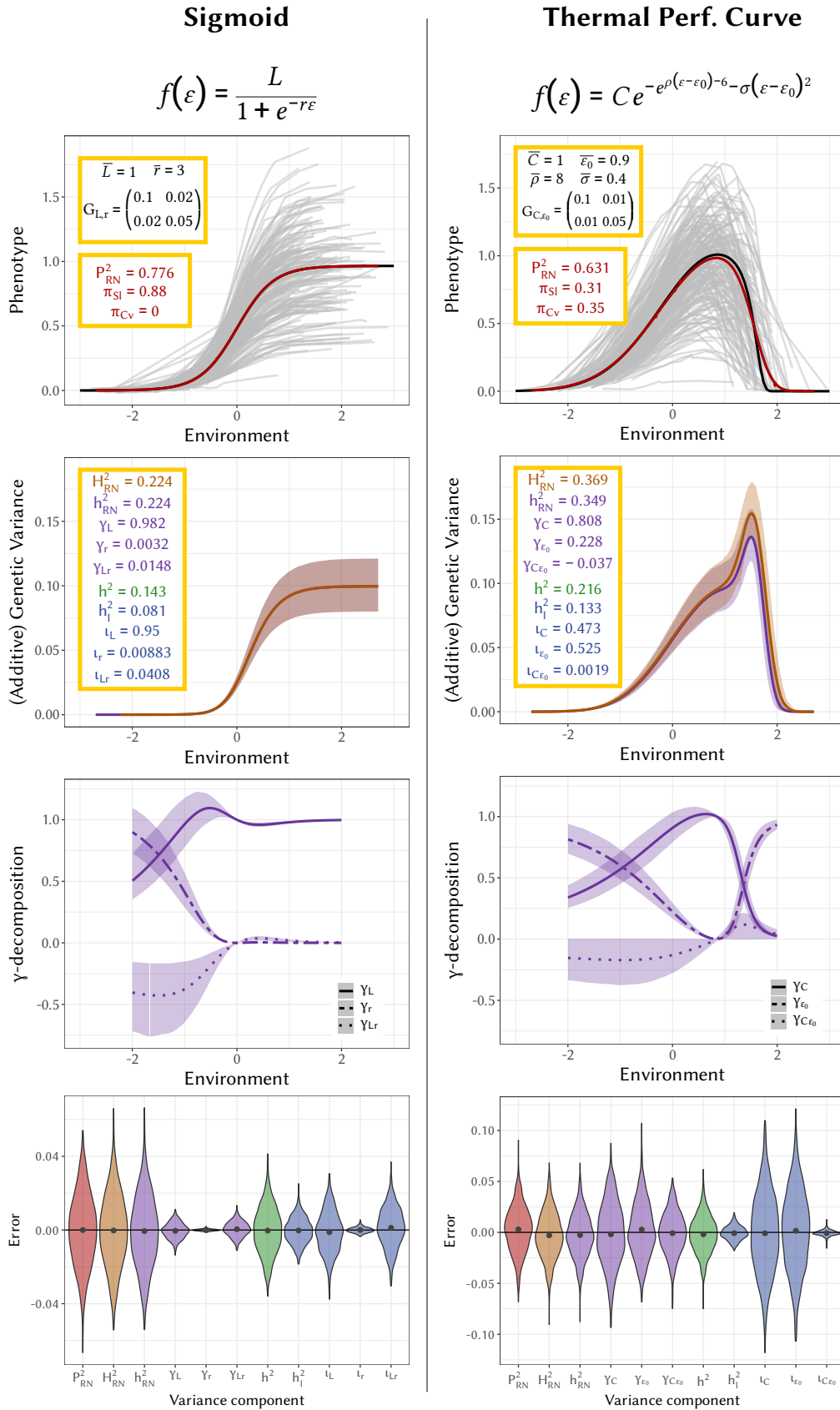


**Figure 6:** Scenarios and results of non-linear modelling of phenotypic plasticity in a continuous environment. On the left: results corresponding to a sigmoid curve scenario; on the right: results corresponding to a TPC scenario. First row: example of the individual curves (each curve corresponds to one individual) simulated in each scenario; yellow box: true parameters for the model and average shape; black curve :  $f(\varepsilon, \theta)$ ; red curve :  $E_{g|\varepsilon}(\hat{z})$ . Second row: distribution of the estimations of  $V_{G,\varepsilon}$  (brown) and  $V_{A,\varepsilon}$  (purple), along the environment; solid line: average value across simulations; pale ribbon: 95% CI across simulations; yellow box: true values for the genetic variance partition. Third row:  $\gamma$ -decomposition of  $V_{A,\varepsilon}$  along the environment, for each parameter and their covariation. Fourth row: distribution of the error for each component of our variance partition (“Variances”) or for the  $\pi$ - and  $\gamma$ -decomposition (“Components”), red dot is the average of estimates over all simulations. 26

541 that the distribution of the environment is different between these two scenarios). It might appear as counter-  
542 intuitive that the slope contributes so much to variance, since the curve increases from 0 and then decreases  
543 toward 0, but this is linked to the fact that the environment is normally distributed, so most values are near  
544  $\varepsilon = 0$ , an area where the slope of the curve is close to [..<sup>69</sup> ]being maximised.

545 Although the variation between genotypes in the top panel of Figure 6 seems quite large, the contribution  
546 from the average plasticity  $\hat{P}_{RN}^2$  is 1.7 to 3.4 times higher than the one of the genetic variance  $\hat{H}_{RN}^2$  (Figure 6,  
547 yellow box in first- and second-row panels). This occurs because the genetic variance is actually very low  
548 in most environments (Figure 6, brown and purple lines of the second-row panels), and scarcely as high as  
549  $V_{Plas}$ . As mentioned above, non-linearity in the parameters is less strong for the sigmoid case than for the  
550 TPC case, resulting in almost exactly equal values for  $\hat{H}_{RN}^2$  and  $\hat{h}_{RN}^2$  for the former, while they are slightly  
551 different for the latter. In both cases, the [..<sup>70</sup> ]small difference between  $\hat{H}_{RN}^2$  and  $\hat{h}_{RN}^2$  can be explained by  
552 the disproportionate importance in the  $\gamma$ -decomposition of parameters that are actually linearly related to  
553 the trait ( $\gamma_L = 0.98$  for the sigmoid and  $\gamma_C = 0.81$  for the TPC scenarios). In terms of heritability [..<sup>71</sup> ]from  
554 plasticity, it is substantial in both cases ( $h_1^2 = 0.081$  for the sigmoid and  $h_1^2 = 0.133$  for the TPC scenario), as  
555 can be expected from the non-parallel reaction norms (Figure 6). However, it remains smaller than the [..<sup>72</sup>  
556 ]environment-blind heritability of the trait in both cases ( $h^2 = 0.143$  for the sigmoid and  $h^2 = 0.216$  for the  
557 TPC scenarios). Interestingly, for the TPC scenario, and contrary to what happens with the  $\gamma$ -decomposition, a  
558 majority of the additive genetic variance [..<sup>73</sup> ]arising from plasticity comes from the variation in the location  
559 of the optimum ( $t_{\varepsilon_0} = 0.525$ ). This is because variation in the location of the optimum shifts the reaction norm  
560 along the environment axis (i.e. on the “x-axis”), meaning that even a small shift can generate considerable  
561 variation that is non-parallel along the phenotype axis (i.e. along the “y-axis”).

562 An interesting aspect of our framework is that we can explore the variation of  $V_{Gen,\varepsilon}$ ,  $V_{A,\varepsilon}$  and the  $\gamma$ -  
563 decomposition of  $V_{A,\varepsilon}$  along the environmental gradient, which can be very informative from an evolutionary  
564 perspective. In the case of the sigmoid curve (Figure 6, second and third rows, left panels), the analysis is  
565 relatively simple : as the value of the environment increases, the parameter  $L$  is multiplied by an increased  
566 value (going from 0 to 1 due to the sigmoid function) and thus its genetic variance plays a stronger role. This  
567 translates into  $V_{Gen,\varepsilon}$  and  $V_{A,\varepsilon}$  increasing with the environment, and  $\gamma_L$  accounting for almost all of the genetic  
568 variance after the sigmoid inflexion point in 0. The TPC scenario is even more interesting. First, we can see  
569 that both  $V_{Gen,\varepsilon}$  and  $V_{A,\varepsilon}$  (Figure 6, second row, right panels) are close to zero in the extreme environments  
570 and maximised in a region between the optimum and critical maximal temperature, where the reaction norm

---

<sup>69</sup> removed: be

<sup>70</sup> removed: low

<sup>71</sup> removed: of

<sup>72</sup> removed: marginal

<sup>73</sup> removed: in

571 suddenly drops after the optimum. This maximum also corresponds to the region where  $V_{\text{Gen},\epsilon}$  and  $V_{\text{A},\epsilon}$  are  
572 the most different (and where the red and black departs the most in [Figure 6](#), top row, right panel). Regarding  
573 the  $\gamma$ -decomposition ([Figure 6](#), third row, right panels), the influence of the location of the optimum ( $\gamma_{\epsilon_0}$ ) is  
574 maximised at extreme environments, while the influence of the maximum value at the peak ( $\gamma_C$ ) is exactly  
575 maximised at the average location of the peak. The influence of the covaration between both ( $\gamma_{C\epsilon_0}$ ) is negative  
576 before the peak and positive after.

577 As these simulations illustrate, our framework allows very finely describing the characteristics of reaction  
578 norms, such as how its average shape (slope/curvature) and genetic variation in the parameters influence the  
579 phenotypic variance in the trait, while discriminating between total genetic variation of the trait and genetic  
580 variation exclusively linked with plasticity itself.

## 581 Discussion

582 The variance decomposition in [Equation 7](#) is very general, and applicable to any approach used to estimate  
583 a reaction norm. In particular, it applies equally well to both the character-state and curve-parameter ap-  
584 proaches. Each component and its variance-standardisation provide a different information on the reaction  
585 norms:  $P_{\text{RN}}^2$  quantifies the proportion of phenotypic variance due to the average plastic response across geno-  
586 types, while  $H_{\text{RN}}^2$  or  $h_{\text{RN}}^2$  quantify the contributions from (broad or additive) genetic variance in the reaction  
587 norms. Further, these genetic components can be separated into the [<sup>74</sup>]environment-blind heritability of  
588 the trait ( $h^2$ ) based on the average breeding values across environments, and the heritability [<sup>75</sup>]from plastic-  
589 ity ( $h_1^2$ ) which is solely based on the gene-by-environment interactions at the level of breeding values. Finally,  
590 the sum  $T_{\text{RN}}^2 = P_{\text{RN}}^2 + H_{\text{RN}}^2$  quantifies how well we can predict the individual phenotypes based on their geno-  
591 types and environments (i.e. genetically variable reaction norms). Those components are efficient summary  
592 statistics yielding important information regarding the evolutionary potential of both the trait and its plastic-  
593 ity. Importantly, they are very generally applicable, with a strict equivalence between e.g. a character-state  
594 or a curve-parameter approach. However, they do not provide information regarding the actual shape of the  
595 reaction norms. To that end, we further decomposed some of these components in terms of characteristics of  
596 the shape or parameters of reaction norms.

597 The most difficult problem is to decompose the average plastic variance  $P_{\text{RN}}^2$  into terms arising either from  
598 the linear trend ( $\pi_{\text{Sl}}$ ) or from the curvature ( $\pi_{\text{Cv}}$ ) of the reaction norm, which we called  $\pi$ -decomposition.  
599 Unfortunately, our estimates for  $\pi_{\text{Sl}}$  and  $\pi_{\text{Cv}}$  are only valid if the environment is normally distributed, or the  
600 true reaction norm is quadratic. In other cases, mean slope and curvature lose their simple interpretation,

---

<sup>74</sup>removed: marginal

<sup>75</sup>removed: of

601 preventing a meaningful  $\pi$ -decomposition. Nonetheless, for polynomial reaction norms of higher order, we  
 602 described an alternative decomposition, based on the polynomial coefficients rather than actual slope and  
 603 curvature, which we called  $\varphi$ -decomposition. While not as interpretable as the  $\pi$ -decomposition, this decom-  
 604 position can serve as a way to compare polynomial shapes across contexts. Based on the equivalence between  
 605 the curve-parameter and character-state, we introduced  $M_{\text{Plas}}^2$  as a way to quantify the ability of a polynomial  
 606 model to recover  $V_{\text{Plas}}$  compared to an “agnostic” model such as the character-state. Our proposed framework  
 607 is summarised in [Figure 3](#).

608 Decomposing  $h_{\text{RN}}^2$  and  $h_I^2$  is comparatively easier, because the model assumed in [Equation 3](#) and [Equation 4](#)  
 609 ensures that we can always translate additive genetic variance in the parameters  $\theta$  into additive genetic vari-  
 610 ance in the trait  $z$ , even if the function  $f$  is not linear in its parameters. Decomposition of the total heritability  
 611 of the reaction norm  $h_{\text{RN}}^2$  into the impact of the parameters  $\theta$  leads to the  $\gamma$ -decomposition. It quantifies the  
 612 relative importance of genetic variance in different reaction norm parameters to the evolvability of the trait.  
 613 For instance if a given selection episode concerns individuals that all experienced the same plasticity-inducing  
 614 environment (i.e. when spatial environmental variation is negligible relative to temporal variation), using the  
 615 multivariate breeder’s equation (Lande 1979), the relative contribution of genetic variation in parameter  $\theta_i$  to  
 616 the response to selection for the trait  $z$  is

$$\frac{\Delta_{\theta_i} \bar{z}}{\Delta \bar{z}} = \gamma_i + \frac{1}{2} \sum_{i \neq j} \gamma_{ij}, \quad (31)$$

617 where the  $\gamma_i$  and  $\gamma_{ij}$  are defined in [Equation 26](#). In other words, the contributions of responses to selection  
 618 by different reaction norm parameters to overall response to selection by the plastic trait  $z$  is directly pro-  
 619 portional to their contribution to its genetic variance. Importantly, these contributions will depend on the  
 620 reaction norm gradient  $\psi_\varepsilon$  defined in [Equation 19](#), and thus on the environment, as illustrated in [Equation 26](#).  
 621 In fact, the environment-specific additive genetic variance  $V_{A,\varepsilon}$  is a critical piece of information regarding  
 622 evolutionary potential, and we can apply the  $\gamma$ -decomposition within each environment as well. For example,  
 623 in the TPC scenario investigated above ([Figure 6](#), right panels), the contribution of the peak height parameter  
 624  $C$  is maximised at the average location of the optimum, where it accounts for 100% of the additive genetic  
 625 variance. On the contrary, the influence of additive genetic variation in the location of the optimum  $\varepsilon_0$  is more  
 626 important in extreme environments. The complex interaction between the role of  $C$  and  $\varepsilon_0$  generates a peak  
 627 for  $V_{A,\varepsilon}$  in the area between the peak and critical maximal value for the environment (where the performance  
 628 curve reaches zero). In the context of predicting eco-evolutionary response to warming, this would mean  
 629 that a slight temperature rise above the optimum would provide a very short window of higher evolvability,  
 630 but followed by a sharp decrease thereof if warming persists. Beyond these simple scenarios, how selection  
 631 acts on reaction norms and plasticity depends on how the environment varies in space and/or time (Scheiner

632 1993b; de Jong 1999; Tufto 2015; King & Hadfield 2019), and how the reaction norm gradient  $\psi_\varepsilon$  and direction  
633 selection on the expressed trait  $z$  covary across environments. However, an in-depth exploration of how to  
634 estimate these selection responses is beyond the scope of the present work.

635 While the  $\gamma$ -decomposition is key to understanding and predicting evolution of the trait, it is based on  
636 the total heritability of the reaction norm  $h_{\text{RN}}^2$ , which combines additive genetic variation in the trait and its  
637 plasticity. To study plasticity in isolation from the [..<sup>76</sup>]environment-blind additive genetic variance in the  
638 trait, we decomposed  $h_{\text{RN}}^2$  in a similar fashion as  $h_{\text{RN}}^2$ , which we called the  $\iota$ -decomposition. The components of  
639 the  $\iota$ -decomposition measure the contribution of each parameter to the evolutionary potential of plasticity, i.e.  
640 to the evolvability of reaction norm shape. In our thermal performance case (TPC) example, the  $\iota$  associated  
641 to  $C$  and  $\varepsilon_0$  were close to 0.5, meaning that evolution can roughly equally impact the peak height  $C$  or the  
642 location of the optimum  $\varepsilon_0$ , should selection on the shape of reaction norms occur.

643 The detailed decomposition that we propose open the door to better [..<sup>77</sup>]comparability across studies,  
644 which can be a challenge in meta-analyses of plasticity. Murren et al. (2014) performed such a meta-analysis,  
645 comparing genetic variation in different parameters of reaction norm shape across published datasets. How-  
646 ever they (i) computed these parameters using only extreme environmental values, instead of the whole range  
647 of environments; (ii) did not account for uneven spacing between environments where relevant; (iii) did not  
648 account for uncertainty in estimations of reaction norms (as previously highlighted by Morrissey & Liefting  
649 2016); and (iv) assumed the modeled reaction norm shape is true. More [..<sup>78</sup>]details about the analyses in that  
650 study [..<sup>79</sup>]are provided in Appendix G. Our approach overcomes all these issues (some of which had been  
651 dealt with already by Morrissey & Liefting 2016; Pélabon et al. 2020). Unfortunately the dataset compiled by  
652 Murren et al. (2014) does not provide information on uncertainty of phenotypic estimates (related to  $V_{\text{Res}}$ ),  
653 precluding proper meta-analysis of reaction norm shape variation.

654 Importantly, our variance partitioning can be implemented through commonly used statistical models,  
655 notably (non-)linear mixed models. We showed that even complex non-linear modelling can perform well,  
656 only at the cost of using dedicated libraries to compute integrals numerically. This means that biologists  
657 can readily seize all the modelling tools introduced here. In particular, although a character-state approach  
658 can be performed using a simple random-intercept model, studies of genetic variance in plasticity seem to  
659 rather use a multi-trait model, which offers more control, but is more difficult to implement (but see Stirling  
660 & Roff 2000). In order to make the variance partitioning introduced here more accessible, we have imple-  
661 mented the computation of [..<sup>80</sup>]all the decomposition mentioned here as an R package named Reacnorm

---

<sup>76</sup>removed: marginal

<sup>77</sup>removed: commensurability and

<sup>78</sup>removed: detail

<sup>79</sup>removed: is

<sup>80</sup>removed:  $\hat{P}_{\text{RN}}^2$  and the heritabilities, as well as their different decompositions as

662 [github.com/devillemereuil/Reacnorm](https://github.com/devillemereuil/Reacnorm), including cases where more than the genetic effect is assumed affect-  
663 ing variation in  $\theta$ . The package also [<sup>81</sup>] provides a tutorial as a vignette, showing how to implement the  
664 models in the Bayesian package brms and use functions from Reacnorm to study the properties of reaction  
665 norms. We hope that this will further stimulate interest in investigating variation and evolutionary potential  
666 of reaction norms.

667 **Code availability** The code for the data simulation and analyses performed in this article is available at  
668 the following repository: [github.com/devillemereuil/CodePartReacnorm](https://github.com/devillemereuil/CodePartReacnorm)

669 **Acknowledgements** We are grateful to Jarrod Hadfield, Thibaut Morel-Journel, Stéphane Robin and John  
670 Stinchcombe for useful discussions and/or comments that much improved the quality of the paper. We thank  
671 the European Research Council (Grant STG-678140-FluctEvol to LMC).

## 672 References

673 Albecker, M. A., Trussell, G. C., & Lotterhos, K. E. (2022) A novel analytical framework to quantify co-gradient  
674 and countergradient variation. *Ecology Letters*, 25:(2022), 1521–1533. doi: [10.1111/ele.14020](https://doi.org/10.1111/ele.14020).

675 Angilletta, M. J. (2009) *Thermal adaptation: a theoretical and empirical synthesis*. OUP Oxford, Jan. 29, 2009.  
676 304 pp.

677 Bates, D., Mächler, M., Bolker, B., & Walker, S. (2015) Fitting linear mixed-effects models using lme4. *Journal*  
678 *of Statistical Software*, 67:(2015), 48.

679 Bonamour, S., Chevin, L.-M., Charmantier, A., & Teplitsky, C. (2019) Phenotypic plasticity in response to  
680 climate change: the importance of cue variation. *Philosophical Transactions of the Royal Society B: Biological*  
681 *Sciences*, 374:(Mar. 18, 2019), 20180178. doi: [10.1098/rstb.2018.0178](https://doi.org/10.1098/rstb.2018.0178).

682 Bradshaw, A. D. (1965) Evolutionary significance of phenotypic plasticity in plants. *Advances in Genetics*. Ed.  
683 by E. W. Caspari & J. M. Thoday. Vol. 13. Cambridge (MA, USA): Academic Press, Jan. 1, 1965, pp. 115–155.  
684 doi: [10.1016/S0065-2660\(08\)60048-6](https://doi.org/10.1016/S0065-2660(08)60048-6).

685 Brown, G. G. & Rutenmiller, H. C. (1977) Means and variances of stochastic vector products with applications  
686 to random linear models. *Management Science*, 24:(Oct. 1977), 210–216. doi: [10.1287/mnsc.24.2.210](https://doi.org/10.1287/mnsc.24.2.210).

687 Bürkner, P.-C. (2017) Advanced bayesian multilevel modeling with the R package brms. *ArXiv170511123 Stat:*(May 31,  
688 2017).

---

<sup>81</sup>removed: included

689 Charmantier, A., McCleery, R. H., Cole, L. R., Perrins, C., Kruuk, L. E. B., & Sheldon, B. C. (2008) Adaptive  
690 phenotypic plasticity in response to climate change in a wild bird population. *Science*, 320:(May 9, 2008),  
691 800–803. doi: [10.1126/science.1157174](https://doi.org/10.1126/science.1157174).

692 Chevin, L.-M., Collins, S., & Lefèvre, F. (2013) Phenotypic plasticity and evolutionary demographic responses  
693 to climate change: taking theory out to the field. *Functional Ecology*, 27:(2013), 967–979. doi: [10.1111/j.1365-2435.2012.02043.x](https://doi.org/10.1111/j.1365-2435.2012.02043.x).

694

695 Chevin, L.-M., Lande, R., & Mace, G. M. (2010) Adaptation, plasticity, and extinction in a changing environment:  
696 towards a predictive theory. *PLOS Biology*, 8:(Apr. 27, 2010), e1000357. doi: [10.1371/journal.pbio.1000357](https://doi.org/10.1371/journal.pbio.1000357).

697 de Jong, G. (1990) Quantitative genetics of reaction norms. *Journal of evolutionary biology*, 3:(1990), 447–468.

698 de Jong, G. (1995) Phenotypic plasticity as a product of selection in a variable environment. *The American*  
699 *Naturalist*, 145:(Apr. 1, 1995), 493–512. doi: [10.1086/285752](https://doi.org/10.1086/285752).

700 de Jong, G. (1999) Unpredictable selection in a structured population leads to local genetic differentiation in  
701 evolved reaction norms. *Journal of Evolutionary Biology*, 12:(1999), 839–851.

702 Des Marais, D. L., Hernandez, K. M., & Juenger, T. E. (2013) Genotype-by-environment interaction and plastic-  
703 ity: exploring genomic responses of plants to the abiotic environment. *Annual Review of Ecology, Evolution,*  
704 *and Systematics*, 44:(2013), 5–29. doi: [10.1146/annurev-ecolsys-110512-135806](https://doi.org/10.1146/annurev-ecolsys-110512-135806).

705 Deutsch, C. A., Tewksbury, J. J., Huey, R. B., Sheldon, K. S., Ghalambor, C. K., Haak, D. C., & Martin, P. R. (2008)  
706 Impacts of climate warming on terrestrial ectotherms across latitude. *Proceedings of the National Academy*  
707 *of Sciences*, 105:(May 6, 2008), 6668–6672. doi: [10.1073/pnas.0709472105](https://doi.org/10.1073/pnas.0709472105).

708 de Villemereuil, P. (2018) Quantitative genetic methods depending on the nature of the phenotypic trait. *An-*  
709 *nals of the New York Academy of Sciences. The Year in Evolutionary Biology* 1422:(June 1, 2018), 29–47. doi:  
710 [10.1111/nyas.13571](https://doi.org/10.1111/nyas.13571).

711 de Villemereuil, P., Morrissey, M. B., Nakagawa, S., & Schielzeth, H. (2018) Fixed-effect variance and the esti-  
712 mation of repeatabilities and heritabilities: issues and solutions. *Journal of Evolutionary Biology*, 31:(2018),  
713 621–632. doi: [10.1111/jeb.13232](https://doi.org/10.1111/jeb.13232).

714 de Villemereuil, P., Schielzeth, H., Nakagawa, S., & Morrissey, M. B. (2016) General methods for evolutionary  
715 quantitative genetic inference from generalised mixed models. *Genetics*, 204:(Nov. 1, 2016), 1281–1294. doi:  
716 [10.1534/genetics.115.186536](https://doi.org/10.1534/genetics.115.186536).

717 de Villemereuil, P. et al. (2020) Fluctuating optimum and temporally variable selection on breeding date in  
718 birds and mammals. *Proceedings of the National Academy of Sciences*, 117:(2020), 31969–31978. doi: [10.1073/pnas.2009003117](https://doi.org/10.1073/pnas.2009003117).

719

720 Falconer, D. S. (1952) The problem of environment and selection. *The American Naturalist*, 86:(Sept. 1, 1952),  
721 293–298. doi: [10.1086/281736](https://doi.org/10.1086/281736).



722 Falconer, D. S. & Mackay, T. F. (1996) *Introduction to quantitative genetics*. 4th ed. Harlow, Essex (UK): Benjamin  
723 Cummings, Feb. 16, 1996.

724 Gavrillets, S. & Scheiner, S. M. (1993a) The genetics of phenotypic plasticity. V. Evolution of reaction norm  
725 shape. *Journal of Evolutionary Biology*, 6:(1993), 31–48. doi: [10.1046/j.1420-9101.1993.6010031.x](https://doi.org/10.1046/j.1420-9101.1993.6010031.x).

726 Gavrillets, S. & Scheiner, S. M. (1993b) The genetics of phenotypic plasticity. VI. Theoretical predictions for  
727 directional selection. *Journal of Evolutionary Biology*, 6:(1993), 49–68.

728 Gienapp, P., Teplitsky, C., Alho, J. S., Mills, J. A., & Merilä, J. (2008) Climate change and evolution: disentangling  
729 environmental and genetic responses. *Molecular Ecology*, 17:(Jan. 1, 2008), 167–178. doi: [10.1111/j.1365-  
730 294X.2007.03413.x](https://doi.org/10.1111/j.1365-294X.2007.03413.x).

731 Gomulkiewicz, R. & Kirkpatrick, M. (1992) Quantitative genetics and the evolution of reaction norms. *Evolu-  
732 tion*, 46:(Apr. 1, 1992), 390–411. doi: [10.1111/j.1558-5646.1992.tb02047.x](https://doi.org/10.1111/j.1558-5646.1992.tb02047.x).

733 Hammill, E., Rogers, A., & Beckerman, A. P. (2008) Costs, benefits and the evolution of inducible defences: a  
734 case study with *Daphnia pulex*. *Journal of Evolutionary Biology*, 21:(May 1, 2008), 705–715. doi: [10.1111/j.  
735 1420-9101.2008.01520.x](https://doi.org/10.1111/j.1420-9101.2008.01520.x).

736 Johnson, J. B. & Omland, K. S. (2004) Model selection in ecology and evolution. *Trends in Ecology & Evolution*,  
737 19:(Feb. 2004), 101–108. doi: [doi:DOI:10.1016/j.tree.2003.10.013](https://doi.org/10.1016/j.tree.2003.10.013).

738 Johnson, P. C. (2014) Extension of Nakagawa & Schielzeth's R2GLMM to random slopes models. *Methods in  
739 Ecology and Evolution*, 5:(Sept. 1, 2014), 944–946. doi: [10.1111/2041-210X.12225](https://doi.org/10.1111/2041-210X.12225).

740 King, J. G. & Hadfield, J. D. (2019) The evolution of phenotypic plasticity when environments fluctuate in time  
741 and space. *Evolution Letters*, 3:(Feb. 1, 2019), 15–27. doi: [10.1002/evl3.100](https://doi.org/10.1002/evl3.100).

742 Kirkpatrick, M. (2009) Patterns of quantitative genetic variation in multiple dimensions. *Genetica*, 136:(June 1,  
743 2009), 271–284. doi: [10.1007/s10709-008-9302-6](https://doi.org/10.1007/s10709-008-9302-6).

744 Kirkpatrick, M. & Heckman, N. (1989) A quantitative genetic model for growth, shape, reaction norms, and  
745 other infinite-dimensional characters. *Journal of Mathematical Biology*, 27:(Aug. 1, 1989), 429–450. doi:  
746 [10.1007/BF00290638](https://doi.org/10.1007/BF00290638).

747 Lande, R. (1979) Quantitative genetic analysis of multivariate evolution, applied to brain:body size allometry.  
748 *Evolution*, 33:(1979), 402–416.

749 Lande, R. (2009) Adaptation to an extraordinary environment by evolution of phenotypic plasticity and genetic  
750 assimilation. *Journal of Evolutionary Biology*, 22:(July 1, 2009), 1435–1446. doi: [10.1111/j.1420-9101.2009.  
751 01754.x](https://doi.org/10.1111/j.1420-9101.2009.01754.x).

752 Lande, R. & Arnold, S. J. (1983) The measurement of selection on correlated characters. *Evolution*, 37:(1983),  
753 1210–1226. doi: [10.2307/2408842](https://doi.org/10.2307/2408842).

- 754 Landsman, Z. & Nešlehová, J. (2008) Stein's Lemma for elliptical random vectors. *Journal of Multivariate Anal-*  
755 *ysis*, 99:(May 1, 2008), 912–927. doi: [10.1016/j.jmva.2007.05.006](https://doi.org/10.1016/j.jmva.2007.05.006).
- 756 Landsman, Z., Vanduffel, S., & Yao, J. (2013) A note on Stein's lemma for multivariate elliptical distributions.  
757 *Journal of Statistical Planning and Inference*, 143:(Nov. 1, 2013), 2016–2022. doi: [10.1016/j.jspi.2013.06.003](https://doi.org/10.1016/j.jspi.2013.06.003).
- 758 Lawley, D. N. (1956) Tests of significance for the latent roots of covariance and correlation matrices. *Biometrika*,  
759 43:(1956), 128–136. doi: [10.2307/2333586](https://doi.org/10.2307/2333586).
- 760 Lynch, M. & Walsh, B. (1998) *Genetics and analysis of quantitative traits*. Sunderland, Massachusetts (US):  
761 Sinauer Associates, 1998.
- 762 Lynch, M. & Gabriel, W. (1987) Environmental tolerance. *The American Naturalist*, 129:(Feb. 1, 1987), 283–303.  
763 doi: [10.1086/284635](https://doi.org/10.1086/284635).
- 764 Merilä, J. & Hendry, A. P. (2014) Climate change, adaptation, and phenotypic plasticity: the problem and the  
765 evidence. *Evolutionary Applications*, 7:(2014), 1–14. doi: [10.1111/eva.12137](https://doi.org/10.1111/eva.12137).
- 766 Mitchell, D. J. & Houslay, T. M. (2021) Context-dependent trait covariances: how plasticity shapes behavioral  
767 syndromes. *Behavioral Ecology*, 32:(Jan. 1, 2021), 25–29. doi: [10.1093/beheco/araa115](https://doi.org/10.1093/beheco/araa115).
- 768 Moczek & Emlen (1999) Proximate determination of male horn dimorphism in the beetle *Onthophagus taurus*  
769 (Coleoptera: Scarabaeidae). *Journal of Evolutionary Biology*, 12:(1999), 27–37. doi: [10.1046/j.1420-9101.](https://doi.org/10.1046/j.1420-9101.1999.00004.x)  
770 [1999.00004.x](https://doi.org/10.1046/j.1420-9101.1999.00004.x).
- 771 Morrissey, M. B. (2015) Evolutionary quantitative genetics of nonlinear developmental systems. *Evolution*,  
772 69:(Aug. 1, 2015), 2050–2066. doi: [10.1111/evo.12728](https://doi.org/10.1111/evo.12728).
- 773 Morrissey, M. B. & Liefting, M. (2016) Variation in reaction norms: Statistical considerations and biological  
774 interpretation. *Evolution*, 70:(Sept. 1, 2016), 1944–1959. doi: [10.1111/evo.13003](https://doi.org/10.1111/evo.13003).
- 775 Murren, C. J., Maclean, H. J., Diamond, S. E., Steiner, U. K., Heskell, M. A., Handelsman, C. A., Ghalambor, C. K.,  
776 Auld, J. R., Callahan, H. S., & Pfennig, D. W. (2014) Evolutionary change in continuous reaction norms. *The*  
777 *American Naturalist*, 183:(2014), 453–467.
- 778 Nakagawa, S. & Schielzeth, H. (2013) A general and simple method for obtaining R<sup>2</sup> from generalized linear  
779 mixed-effects models. *Methods in Ecology and Evolution*, 4:(2013), 133–142. doi: [10.1111/j.2041-210x.2012.](https://doi.org/10.1111/j.2041-210x.2012.00261.x)  
780 [00261.x](https://doi.org/10.1111/j.2041-210x.2012.00261.x).
- 781 Narasimhan, B., Johnson, S. G., Hahn, T., Bouvier, A., & Kiêu, K. (2023) *Cubature: Adaptive multivariate inte-*  
782 *gration over hypercubes*. manual. 2023.
- 783 Nussey, D. H., Wilson, A. J., & Brommer, J. E. (2007) The evolutionary ecology of individual phenotypic  
784 plasticity in wild populations. *Journal of Evolutionary Biology*, 20:(2007), 831–844. doi: [10.1111/j.1420-](https://doi.org/10.1111/j.1420-9101.2007.01300.x)  
785 [9101.2007.01300.x](https://doi.org/10.1111/j.1420-9101.2007.01300.x).

786 Nussey, D. H., Postma, E., Gienapp, P., & Visser, M. E. (2005) Selection on heritable phenotypic plasticity in a  
787 wild bird population. *Science*, 310:(Oct. 14, 2005), 304–306. doi: [10.1126/science.1117004](https://doi.org/10.1126/science.1117004).

788 Pélabon, C., Hilde, C. H., Einum, S., & Gamelon, M. (2020) On the use of the coefficient of variation to quantify  
789 and compare trait variation. *Evolution Letters*:(2020). doi: [10.1002/evl3.171](https://doi.org/10.1002/evl3.171).

790 Pinheiro, J., Bates, D., DebRoy, S., Sarkar, D., & {the R Core team} (2009) *Nlme: Linear and Nonlinear Mixed*  
791 *Effects Models*. 2009.

792 Reed, T. E., Waples, R. S., Schindler, D. E., Hard, J. J., & Kinnison, M. T. (2010) Phenotypic plasticity and  
793 population viability: the importance of environmental predictability. *Proceedings of the Royal Society B:*  
794 *Biological Sciences*, 277:(Nov. 22, 2010), 3391–3400. doi: [10.1098/rspb.2010.0771](https://doi.org/10.1098/rspb.2010.0771).

795 Rice, S. H. (2004) *Evolutionary Theory: Mathematical and Conceptual Foundations*. Sinauer, Sept. 1, 2004. 348 pp.

796 Robertson, A. (1966) A mathematical model of the culling process in dairy cattle. *Animal Science*, 8:(1966),  
797 95–108. doi: [10.1017/S0003356100037752](https://doi.org/10.1017/S0003356100037752).

798 Rovelli, G. et al. (2020) The genetics of phenotypic plasticity in livestock in the era of climate change: a review.  
799 *Italian Journal of Animal Science*, 19:(Dec. 14, 2020), 997–1014. doi: [10.1080/1828051X.2020.1809540](https://doi.org/10.1080/1828051X.2020.1809540).

800 Schaum, C. E. & Collins, S. (2014) Plasticity predicts evolution in a marine alga. *Proceedings of the Royal Society*  
801 *B: Biological Sciences*, 281:(Oct. 22, 2014), 20141486. doi: [10.1098/rspb.2014.1486](https://doi.org/10.1098/rspb.2014.1486).

802 Scheiner, S. M. (1993a) Genetics and evolution of phenotypic plasticity. *Annual Review of Ecology and System-*  
803 *atics*, 24:(Nov. 1993), 35–68. doi: [10.1146/annurev.es.24.110193.000343](https://doi.org/10.1146/annurev.es.24.110193.000343).

804 Scheiner, S. M. (1993b) Plasticity as a selectable trait: reply to Via. *The American Naturalist*, 142:(Aug. 1, 1993),  
805 371–373. doi: [10.1086/285544](https://doi.org/10.1086/285544).

806 Scheiner, S. M. & Lyman, R. F. (1989) The genetics of phenotypic plasticity I. Heritability. *Journal of Evolution-*  
807 *ary Biology*, 2:(Mar. 1989), 95–107. doi: [10.1046/j.1420-9101.1989.2020095.x](https://doi.org/10.1046/j.1420-9101.1989.2020095.x).

808 Schlichting, C. D. & Pigliucci, M. (1998) Phenotypic evolution: a reaction norm perspective. *Phenotypic evolu-*  
809 *tion: a reaction norm perspective*:(1998).

810 Stinchcombe, J. R., Function-valued Traits Working Group, & Kirkpatrick, M. (2012) Genetics and evolution  
811 of function-valued traits: understanding environmentally responsive phenotypes. *Trends in Ecology &*  
812 *Evolution*, 27:(Nov. 1, 2012), 637–647. doi: [10.1016/j.tree.2012.07.002](https://doi.org/10.1016/j.tree.2012.07.002).

813 Stirling, G. & Roff, D. A. (2000) Behaviour plasticity without learning: phenotypic and genetic variation of  
814 naïve *Daphnia* in an ecological trade-off. *Animal Behaviour*, 59:(May 1, 2000), 929–941. doi: [10.1006/anbe.](https://doi.org/10.1006/anbe.1999.1386)  
815 [1999.1386](https://doi.org/1999.1386).

816 Suzuki, Y. & Nijhout, H. F. (2006) Evolution of a polyphenism by genetic accommodation. *Science*, 311:(Feb. 3,  
817 2006), 650–652. doi: [10.1126/science.1118888](https://doi.org/10.1126/science.1118888).

- 818 Teplitsky, C., Mills, J. A., Alho, J. S., Yarrall, J. W., & Merilä, J. (2008) Bergmann's rule and climate change  
819 revisited: Disentangling environmental and genetic responses in a wild bird population. *Proceedings of the*  
820 *National Academy of Sciences*, 105:(Sept. 9, 2008), 13492–13496. doi: [10.1073/pnas.0800999105](https://doi.org/10.1073/pnas.0800999105).
- 821 Tredennick, A. T., Hooker, G., Ellner, S. P., & Adler, P. B. (2021) A practical guide to selecting models for  
822 exploration, inference, and prediction in ecology. *Ecology*, 102:(2021), e03336. doi: [10.1002/ecy.3336](https://doi.org/10.1002/ecy.3336).
- 823 Tufto, J. (2000) The evolution of plasticity and nonplastic spatial and temporal adaptations in the presence of  
824 imperfect environmental cues. *The American Naturalist*, 156:(Aug. 1, 2000), 121–130. doi: [10.1086/303381](https://doi.org/10.1086/303381).
- 825 Tufto, J. (2015) Genetic evolution, plasticity, and bet-hedging as adaptive responses to temporally autocorre-  
826 lated fluctuating selection: A quantitative genetic model. *Evolution*, 69:(2015), 2034–2049. doi: [10.1111/evo.](https://doi.org/10.1111/evo.12716)  
827 [12716](https://doi.org/10.1111/evo.12716).
- 828 Vedder, O., Bouwhuis, S., & Sheldon, B. C. (2013) Quantitative assessment of the importance of phenotypic  
829 plasticity in adaptation to climate change in wild bird populations. *PLOS Biology*, 11:(2013), e1001605. doi:  
830 [10.1371/journal.pbio.1001605](https://doi.org/10.1371/journal.pbio.1001605).
- 831 Via, S. & Lande, R. (1985) Genotype-environment interaction and the evolution of phenotypic plasticity. *Evo-*  
832 *lution*, 39:(May 1, 1985), 505–522. doi: [10.1111/j.1558-5646.1985.tb00391.x](https://doi.org/10.1111/j.1558-5646.1985.tb00391.x).
- 833 Wilson, A. J., Réale, D., Clements, M. N., Morrissey, M. M., Postma, E., Walling, C. A., Kruuk, L. E. B., & Nussey,  
834 D. H. (2010) An ecologist's guide to the animal model. *Journal of Animal Ecology*, 79:(Jan. 2010), 13–26.  
835 doi: [10.1111/j.1365-2656.2009.01639.x](https://doi.org/10.1111/j.1365-2656.2009.01639.x).
- 836 Woltereck, R. (1909) Weitere experimentelle Untersuchungen über Artveränderung, speziell über das Wesen  
837 quantitativer Artunterschiede bei Daphniden. *Verh. D. Tsch. Zool. Ges.*, 1909:(1909), 110–172.

# Appendix

838

## A A unified formalism for the curve-parameters and character-state approaches

840

841 Despite having different mechanics, the curve-parameter and character-state approaches can be shown to  
842 be mathematically equivalent de Jong (1995). We can use this to express both approaches under the same,  
843 unified formalism. More precisely, we can express the character-state approach as being a special case of the  
844 curve-parameters approach. Under a curve-parameters approach, the reaction norm is seen as a function  $f$   
845 of the environment  $\varepsilon$  and a vector of parameters  $\theta_g$ :

$$\hat{z} = f(\varepsilon, \theta_g). \quad (\text{S1})$$

846 The  $\theta_g$ 's covary across genotypes with a variance-covariance matrix  $G_\theta$ :

$$\theta_g \sim \mathcal{N}(\bar{\theta}, G_\theta). \quad (\text{S2})$$

847 By contrast, in a character-state approach, the reaction norm values of different genotypes across environ-  
848 ments are directly provided by sampling from a multivariate normal distribution:

$$\hat{z} \sim \mathcal{N}(\boldsymbol{\mu}, G_z). \quad (\text{S3})$$

849 One way to express the character-state using the same formalism as the curve-parameter is to recognise that  
850 [Equation S3](#) can be written as

$$\begin{aligned} \hat{z} &= \boldsymbol{\mu}_g^T \mathbf{u}_k, \\ \boldsymbol{\mu}_g &\sim \mathcal{N}(\boldsymbol{\mu}, G_z), \end{aligned} \quad (\text{S4})$$

851 where  $\mathbf{u}_k$  is the unit vector with 1 at the  $k$ th value (corresponding to environment  $\varepsilon_k$ ) and 0 elsewhere. Thus,  
852 the character-state model can be expressed using the formalism of [Equation S1](#) and [Equation S2](#), where  $\boldsymbol{\mu}_g$  in  
853 [Equation S4](#) plays the role of  $\theta_g$ , and thus  $G_z$  plays the role of  $G_\theta$ . In this case, the function  $f$  is a function  
854 taking the level  $k$  of the environment and the parameters  $\boldsymbol{\mu}_g$  of the genotype  $g$  as input, and yielding the  
855 evaluated reaction norm  $\hat{z}$  as the output. Evidently, this function  $f$  is not continuous and not differentiable  
856 along the (categorical) environment. However, it is a continuous, differentiable and even linear function  
857 along the (continuous) parameters  $\boldsymbol{\mu}_g$ . As such, all properties mentioned in the main text and the Appendices  
858 pertaining to reaction norms that are “linear in its parameters” also apply to the character-state approach.

859 **B Computation of the additive genetic variance holding**  
 860 **environment constant**

861 **B1 Preliminary results**

862 **Multiple regression slopes expressed using a variance-covariance matrix** Let us assume a multiple  
 863 regression between a random variable  $y$  and a set of random variables  $\mathbf{x} = (x_1, \dots, x_n)^T$  such that:

$$y = \mu + \mathbf{x}^T \boldsymbol{\beta} + e, \quad (\text{S5})$$

864 where  $\mu$  is the intercept and  $e$  is the residual of the model. Note that in practical regression, the realised  
 865 sampling of  $\mathbf{x}$  will be contained in the design matrix of the model. If it exists and is unique, the solution for  
 866 the vector of multiple regression slopes  $\boldsymbol{\beta}$  can be formulated in terms variance-covariance matrices (see e.g.  
 867 p.179, Lynch & Walsh 1998):

$$\boldsymbol{\beta} = V(\mathbf{x})^{-1} \text{cov}(\mathbf{x}, y), \quad (\text{S6})$$

868 where  $V(\mathbf{x})$  is the variance-covariance matrix of  $\mathbf{x}$ ,  $V(\mathbf{x})^{-1}$  is its inverse matrix and  $\text{cov}(\mathbf{x}, y)$  is the column-  
 869 vector of covariances between the  $x_i$  and  $y$ .

870 **Multivariate version of Stein's lemma** Let us assume that  $\mathbf{x} = (x_1, \dots, x_{p_x})$  and  $\mathbf{y} = (y_1, \dots, y_{p_y})$  follow  
 871 multivariate normal distributions, and that  $g$  is a differentiable,  $R^{p_x} \rightarrow R$  function such that  $E(\nabla g)$ , where  
 872  $\nabla g$  is the gradient of  $g$  (the vector of partial derivatives), is a vector with finite values, then it can be shown  
 873 (Landsman & Nešlehová 2008; Landsman et al. 2013) that:

$$\text{cov}(g(\mathbf{x}), y) = \text{cov}(\mathbf{x}, y) E(\nabla g). \quad (\text{S7})$$

874 Note that covariance matrices of vectors (also known as cross-covariance matrices) are not commutative, but  
 875 are such that  $\text{cov}(\mathbf{x}, y) = \text{cov}(y, \mathbf{x})^T$ . In the case where  $p_y = 1$ , then  $y = y$  follows a normal distribution and:

$$\text{cov}(g(\mathbf{x}), y) = \text{cov}(y, \mathbf{x}) E(\nabla g). \quad (\text{S8})$$

876 Note that  $\text{cov}(y, \mathbf{x})$  is a row-vector and  $\text{cov}(\mathbf{x}, y)$  is a column-vector by convention.

## 877 **B2 Breeding values in a given environment**

878 **Genetics of reaction norms** As mentioned in the main text, a general formalism (including the character-  
879 state as a special case) for the reaction norm  $\hat{z}$  is given by [Equation 3](#) in the main text, i.e.

$$\hat{z} = f(\varepsilon, \theta_g). \quad (\text{S9})$$

880 The phenotype predicted by the reaction norm  $\hat{z}$  thus depends on the environmental value  $\varepsilon$ , and the reac-  
881 tion norm parameters  $\theta_g$  specific to the genotype  $g$ . When holding the environment  $\varepsilon$  constant, the genetic  
882 variance is simply the variance of reaction norms across genotypes:

$$V_{G|\varepsilon} = V_{g|\varepsilon} (f(\varepsilon, \theta_g)) \quad (\text{S10})$$

883 If the reaction norms are estimated in such a way that non-additive genetic variance can be separated out from  
884 additive genetic variance (e.g. if “genotype” refers to individuals) or are known to be negligible on the one  
885 hand; and if the reaction norm is linear in its parameters (i.e.  $f$  is a linear function of  $\theta_g$ , as for a polynomial  
886 function) on the other hand, then the additive genetic variance conditional on the environment is readily  
887 given by [Equation S10](#), i.e.  $V_{A|\varepsilon} = V_{G|\varepsilon}$ . In the case where  $f$  is not linear in its parameters, it is necessary to  
888 rely on the theory in non-linear quantitative genetics (Morrissey 2015; de Villemereuil et al. 2016), as we do  
889 below.

890 **Linear relationship between breeding values** The relationship between the breeding value of the trait  
891  $\mathcal{A}_z$  and the breeding values of the reaction norm parameters  $\theta_g$  is the key towards developing a framework  
892 that works for any reaction norm, linear in its parameters or not. Let us note  $\mathcal{A}_\theta$  the vector of breeding values  
893 of all the parameters in  $\theta$ . We will follow the same demonstration as in de Villemereuil et al. (2016), which  
894 starts from the point that, by definition, breeding values are all linked through linear relationships (see also  
895 Robertson 1966), since they are all linearly linked to the genotype (Lynch & Walsh 1998). More precisely, the  
896 breeding value  $\mathcal{A}_z$  of the phenotypic trait  $z$  of an individual linearly depends on a linear combination of its  
897 breeding values for the reaction norm parameters  $\mathcal{A}_\theta$ , so that:

$$\mathcal{A}_z = \mu_{\mathcal{A}} + \mathcal{A}_\theta^T \boldsymbol{\psi} \quad (\text{S11})$$

898 where  $\mu_{\mathcal{A}}$  is a constant chosen such that  $E(\mathcal{A}_z) = 0$ ,  $\boldsymbol{\psi}$  is a vector of slopes that we will shortly describe as the  
899 reaction norm gradient.

900 **Derivation of  $\boldsymbol{\psi}$**  To derive an expression of  $\boldsymbol{\psi}$ , we can apply the results in [Equation S6](#) to [Equation S11](#),  
 901 yielding

$$\boldsymbol{\psi} = \mathbf{G}_\theta^{-1} \text{cov}(\mathcal{A}_\theta, \hat{z}). \quad (\text{S12})$$

902 This assumes that  $\text{cov}(\mathcal{A}_\theta, \mathcal{A}_z) = \text{cov}(\mathcal{A}_\theta, \hat{z})$ , i.e. that there is no covariance between the environmental  
 903 values of the phenotype as predicted by the reaction norm and the breeding values of the parameters. This  
 904 results also assumes that  $\mathbf{G}_\theta$  is invertible. However, such assumption is already necessary to most statistical  
 905 algorithms available to infer  $\mathbf{G}_\theta$  in practice, so that this assumption is not limiting here. Noting that  $\hat{z} = f(\varepsilon, \boldsymbol{\theta})$ ,  
 906 we can apply the multivariate version of Stein's lemma ([Equation S7](#)):

$$\boldsymbol{\psi} = \mathbf{G}_\theta^{-1} \text{cov}(\mathcal{A}_\theta, \boldsymbol{\theta}_g) \mathbf{E}(\nabla_\theta f) = \mathbf{G}_\theta^{-1} \mathbf{G}_\theta \mathbf{E}(\nabla_\theta f) = \mathbf{E}(\nabla_\theta f), \quad (\text{S13})$$

907 where we have used the fact that the covariance of breeding values of reaction norm parameters with their  
 908 breeding values is their additive genetic covariance matrix  $\mathbf{G}_\theta$ . Again, note that this assumes that  $f$  is partially  
 909 differentiable with respect to all elements of  $\boldsymbol{\theta}_g$ . Given that this demonstration was applied when holding the  
 910 environment constant, the values in  $\boldsymbol{\psi}$  generally depend on the environment  $\varepsilon$ , so below and in the main text,  
 911 we use the notation  $\boldsymbol{\psi}_\varepsilon$ .

912 **Values of  $\boldsymbol{\psi}_\varepsilon$  in specific contexts** When the reaction norm is linear in its parameters, the values in  $\boldsymbol{\psi}_\varepsilon$  are  
 913 (trivially) the linear coefficients of such relation. For a quadratic reaction norm, where  $\hat{z} = (\bar{\mathcal{A}} + a_g) + (\bar{b} + b_g)\varepsilon +$   
 914  $(\bar{c} + c_g)\varepsilon^2$ , such linear coefficients are respectively 1,  $\varepsilon$  and  $\varepsilon^2$  for  $a_g$ ,  $b_g$  and  $c_g$ . It results that  $\boldsymbol{\psi}_\varepsilon = (1, \varepsilon, \varepsilon^2)^T$   
 915 as mentioned in the main text. More generally, if  $f$  is a polynomial of order  $N$ , then  $\boldsymbol{\psi}_\varepsilon = (1, \varepsilon, \dots, \varepsilon^N)^T$ . In  
 916 the context of a character-state, it can be seen from [Equation S4](#) that the gradient  $\boldsymbol{\psi}_\varepsilon$  in the parameters will be  
 917 equal to  $\mathbf{u}_k$ , i.e. a vector of 1 for the  $k$ th value (corresponding to the environment chosen to be hold constant)  
 918 and 0 elsewhere.

### 919 **B3 Additive genetic variance**

920 By definition, the additive genetic variance of the trait conditional on the environment  $V_{A|\varepsilon}$  is the variance of  
 921 the breeding values defined in [Equation S11](#). We can thus express it from the breeding values of the reaction  
 922 norm parameters (right hand side of [Equation S11](#)) as

$$V_{A|\varepsilon} = \mathbf{V}_{g|\varepsilon}(\mathcal{A}_\theta^T \boldsymbol{\psi}_\varepsilon) = \boldsymbol{\psi}_\varepsilon^T \mathbf{G}_\theta \boldsymbol{\psi}_\varepsilon. \quad (\text{S14})$$

923 This formula holds whether the reaction norm is linear on its parameters or not, and also holds for the  
 924 character-state approach (although in this case, this formula merely selects the  $k$ th element of the diagonal



925 of  $G_z$ ).

## 926 **C Derivation of the general decomposition of variance**

### 927 **C1 Distinguishing between $V_{\text{Plas}}$ , $V_{\text{Gen}}$ and $V_{\text{Add}}$**

928 The phenotype predicted by the reaction norm  $\hat{z}$  depends on the environment, and the reaction norm param-  
929 eters  $\theta_g$  specific to the genotype  $g$ . The impacts of environment and genotype are intricately related via the  
930 reaction norm shape, but in a given environment, one can still isolate the average impact of the environment  
931 from variation among genotypes by computing the average value of the reaction norm across genotypes con-  
932 ditional on the environment, i.e.  $E_{g|\varepsilon}(\hat{z})$ . The variance of  $E_{g|\varepsilon}(\hat{z})$ , taken across environments, is the component  
933  $V_{\text{Plas}} = V(E_{g|\varepsilon}(\hat{z}))$  in the main text, i.e. the phenotypic variance arising from plasticity after averaging across  
934 genotypes. The genotypic value  $\mathcal{G}_z$  of genotype  $g$  within the environment  $\varepsilon$  is then given by

$$\mathcal{G}_z = \hat{z} - E_{g|\varepsilon}(\hat{z}). \quad (\text{S15})$$

935 Note that, although we removed the average effect of the environment, the genotypic value  $\mathcal{G}_z$  still depends on  
936 both the genotype  $g$  and the environment  $\varepsilon$ , because genotypes can vary in their response to the environment.  
937 The total genetic variance in the reaction norm is thus  $V_{\text{Gen}} = V(\mathcal{G}_z)$ . It is possible to get to the breeding values  
938 of the trait in each environment  $\mathcal{A}_z$  following the process described in [Appendix B](#), i.e.  $\mathcal{A}_z = \mu_a + \mathcal{A}_\theta^T \psi_\varepsilon$ . The  
939 total additive genetic variance in the reaction norm is then

$$V_{\text{Add}} = V(\mathcal{A}_z) = E(V_{g|\varepsilon}(\mathcal{A}_z)) + V(E_{g|\varepsilon}(\mathcal{A}_z)) = E(\psi_\varepsilon^T G_\theta \psi_\varepsilon), \quad (\text{S16})$$

940 using the law of total variance and noting that  $E_{g|\varepsilon}(\mathcal{A}_z) = 0$  by construction. In [Figure 1](#) in the main text,  
941 the average  $E_{g|\varepsilon}(\hat{z})$  corresponds to the red line in the left panel of [Figure 1](#) in the main text, while  $\mathcal{A}_z$   
942 corresponds to the purple lines in the middle panel.

### 943 **C2 Distinguishing between $V_{\text{Add}}$ , $V_A$ and $V_{A \times E}$**

944 We can separate the total additive genetic variance of the reaction norm,  $V_{\text{Add}}$ , into two components: the [<sup>82</sup>  
945 ]environment-blind additive genetic variance of the trait  $V_A$  and the additive genetic variance [<sup>83</sup>] arising  
946 from plasticity  $V_{A \times E}$ . The first component is given by considering, for a given genotype, its average breeding

---

<sup>82</sup>removed: marginal

<sup>83</sup>removed: of

947 value across environment:

$$\bar{\mathcal{A}} = E_{\varepsilon|g}(\mathcal{A}_z). \quad (\text{S17})$$

948 This average corresponds to the breeding value that would be predicted for the same genotype present in all  
 949 environments (or moving across them, being measured several times), ignoring the impact of the environment.  
 950 In other words, this average is the predicted breeding value after the impact of the environment has been  
 951 marginalised. Graphically, it depicts the average shift in the  $y$ -axis of the reaction norm, as can be seen in the  
 952 middle panel of [Figure 1](#) in the main text. The [<sup>84</sup>]environment-blind additive genetic variance of the trait  
 953 is

$$V_A = V(\bar{\mathcal{A}}) = E(\boldsymbol{\psi}_\varepsilon)^T G_\theta E(\boldsymbol{\psi}_\varepsilon) \quad (\text{S18})$$

954  $V_A$  is here defined as a variance, but there are negative elements in  $E(\boldsymbol{\psi}_\varepsilon)$  and  $G_\theta$ , so in theory, their product  
 955 could happen to be a negative scalar. This is not so here, because  $G_\theta$  being a variance-covariance matrix, it  
 956 must be positive semi-definite. By definition of positive semi-definiteness, the product  $E(\boldsymbol{\psi}_\varepsilon)^T G_\theta E(\boldsymbol{\psi}_\varepsilon)$  will  
 957 be positive (or null) for any real vector  $E(\boldsymbol{\psi}_\varepsilon)$ .

958 The remaining additive genetic variation after accounting for the marginal breeding value is linked to  
 959 the impact of genetic variation [<sup>85</sup>]arising from plasticity, i.e. genotype-by-environment interactions. We  
 960 can define the part of the breeding values strictly linked to that genotype-by-environment interaction by  
 961 mean-centring the breeding values, for each genotype:

$$\mathcal{A}_I = \mathcal{A}_z - \bar{\mathcal{A}}. \quad (\text{S19})$$

962 The right panel of [Figure 1](#) depicts these interaction breeding values. The additive genetic variance linked to  
 963 genotype-by-environment, and thus to variation [<sup>86</sup>]arising from plasticity, is:

$$V_{A \times E} = V(\mathcal{A}_I) = V(\mathcal{A}_z) + V(\bar{\mathcal{A}}) - 2\text{cov}(\mathcal{A}_z, \bar{\mathcal{A}}) = V(\mathcal{A}_z) - V(\bar{\mathcal{A}}) = V_{\text{Add}} - V_A, \quad (\text{S20})$$

964 noting that, by construction,  $\text{cov}(\mathcal{A}_z, \bar{\mathcal{A}}) = \text{cov}(\bar{\mathcal{A}}, \bar{\mathcal{A}}) = V(\bar{\mathcal{A}})$ . By substituting  $V_{\text{Add}}$  and  $V_A$  with their  
 965 values in [Equation S16](#) and [Equation S18](#), we obtain

$$V_{A \times E} = E(\boldsymbol{\psi}_\varepsilon^T G_\theta \boldsymbol{\psi}_\varepsilon) - E(\boldsymbol{\psi}_\varepsilon)^T G_\theta E(\boldsymbol{\psi}_\varepsilon) = \text{tr}(\Psi G_\theta) = \sum_{l,k} \Psi_{l,k} G_{\theta(l,k)}, \quad (\text{S21})$$

966 where  $\Psi$  is the variance-covariance matrix of the reaction norm gradient  $\boldsymbol{\psi}_\varepsilon$  across the environment. In other

---

<sup>84</sup>removed: marginal

<sup>85</sup>removed: in plasticity, arising from

<sup>86</sup>removed: in

967 words,  $V_{A \times E}$  is the sum of the products, for all pairs of parameters, of the (co)variance in the reaction norm  
 968 gradient and the additive genetic (co)variance. The  $\gamma$ - and  $\iota$ -decomposition directly comes from dividing each  
 969 elements of the sums in Equation S16 and Equation S21 respectively by  $V_{\text{Add}}$  and  $V_{A \times E}$ , so that the total sums  
 970 to 1.

### 971 C3 Variance decomposition for a polynomial model

972 In this section, we will assume a polynomial reaction norm:

$$\hat{z} = \sum_{n=0}^N (\bar{\theta}_n + \theta_{n,g}) \varepsilon^n \quad (\text{S22})$$

973 where  $\theta_n = \bar{\theta}_n + \theta_{n,g}$  is the  $n$ th order coefficient of the polynomial. In this form, it is easy to remark that  
 974 polynomial reaction norms are linear in their parameters, i.e. there is a linear relationship between the  $\theta_n$ 's  
 975 and  $\hat{z}$ , so that  $\mathcal{G}_z = \mathcal{A}_z$ . It results that:

$$\mathcal{G}_z = \mathcal{A}_z = \hat{z} - E_{g|\varepsilon}(\hat{z}) = \sum_{n=0}^N (\bar{\theta}_n + \theta_{n,g}) \varepsilon^n - \sum_{n=0}^N \bar{\theta}_n \varepsilon^n = \sum_{n=0}^N \theta_{n,g} \varepsilon^n. \quad (\text{S23})$$

976 Taking the derivative of this expression with respect to each of  $\theta_{n,g}$  in a given environment  $\varepsilon$  would yield a  
 977 reaction norm gradient equal to the value of each exponent of  $\varepsilon$ , i.e.  $\boldsymbol{\psi}_\varepsilon = (1, \varepsilon, \dots, \varepsilon^N)^T$ . The total (additive)  
 978 genetic variance is thus:

$$V_{\text{Gen}} = V_{\text{Add}} = E(\boldsymbol{\psi}_\varepsilon^T \mathcal{G}_\theta \boldsymbol{\psi}_\varepsilon) = \sum_n V_n E(\varepsilon^{2n}) + 2 \sum_{n < m} C_{nm} E(\varepsilon^{n+m}), \quad (\text{S24})$$

979 where  $V_n$  is the additive genetic variance for  $\theta_{n,g}$  and  $C_{nm}$  is the additive genetic covariance between  $\theta_{m,g}$  and  
 980  $\theta_{n,g}$ . For the quadratic case, if  $\varepsilon$  has been mean-centred and is symmetrical, we have  $E(\varepsilon) = E(\varepsilon^3) = 0$  and the  
 981 expression reduces to

$$V_{\text{Gen}} = V_{\text{Add}} = V_0 + (V_1 + C_{03})E(\varepsilon^2) + V_3E(\varepsilon^4). \quad (\text{S25})$$

982 For a given genotype, its average breeding value across environments is

$$\bar{\mathcal{A}} = E_{\varepsilon|g}(\mathcal{A}_z) = E_{\varepsilon|g} \left( \sum_{n=0}^N \theta_{n,g} \varepsilon^n \right) = \sum_{n=0}^N \theta_{n,g} E(\varepsilon^n) \quad (\text{S26})$$

983 The [<sup>87</sup>]environment-blind (additive) genetic variance of the trait is

$$V_G = V_A = E(\boldsymbol{\psi}_\varepsilon)^T \mathcal{G}_\theta E(\boldsymbol{\psi}_\varepsilon) = \sum_n V_n E(\varepsilon^n)^2 + 2 \sum_{n < m} C_{nm} E(\varepsilon^n) E(\varepsilon^m) \quad (\text{S27})$$

---

<sup>87</sup>removed: marginal

984 For the quadratic case with mean-centred and symmetrical  $\varepsilon$ , this yields:

$$V_A = V_0 + 2C_{02}E(\varepsilon^2) + V_2E(\varepsilon^2)^2 \quad (\text{S28})$$

985 Finally, the additive genetic variance [<sup>88</sup>] arising from plasticity itself is

$$V_{A \times E} = V_{\text{Add}} - V_A = \sum_n V_n E(\varepsilon^{2n}) + 2 \sum_{n < m} C_{nm} E(\varepsilon^{n+m}) - \sum_n V_n E(\varepsilon^n)^2 + 2 \sum_{n < m} C_{nm} E(\varepsilon^n) E(\varepsilon^m). \quad (\text{S29})$$

986 By recognising that  $V(\varepsilon^n) = E(\varepsilon^{2n}) - E(\varepsilon^n)^2$  and  $\text{cov}(\varepsilon^n, \varepsilon^m) = E(\varepsilon^{n+m}) - E(\varepsilon^n)E(\varepsilon^m)$ , we can further simplify  
987 this expression as:

$$V_{A \times E} = \sum_n V_n V(\varepsilon^n) + 2 \sum_{lk} C_{nm} \text{cov}(\varepsilon^n, \varepsilon^m). \quad (\text{S30})$$

988 For the quadratic case, for a mean-centred and symmetrical  $\varepsilon$ , all the covariances between the different expo-  
989 nents of  $\varepsilon$  are 0, yielding

$$V_{A \times E} = V_1 V(\varepsilon) + V_2 V(\varepsilon^2). \quad (\text{S31})$$

## 990 C4 Variance decomposition for the character-state approach

991 As mentioned in [Appendix A](#), the character-state can be written using a function  $f$  such that in environment  
992  $\varepsilon_k$  and for genotype  $g$ , we have

$$\hat{z} = f(\boldsymbol{\mu}_g, \varepsilon_k) = \boldsymbol{\mu}_g^T \mathbf{u}_k. \quad (\text{S32})$$

993 In a given environment  $\varepsilon_k$ , the unit vector  $\mathbf{u}_k$  is equal to 1 at the  $k$ th index and 0 elsewhere. The reaction  
994 norm gradient is equal to this unit vector, i.e.  $\boldsymbol{\psi}_{\varepsilon_k} = \mathbf{u}_k$ . In the first environment, for example, we have  
995  $\boldsymbol{\psi}_{\varepsilon_1} = \mathbf{u}_1 = (1, 0, \dots)^T$ . As mentioned in [Appendix A](#), the character-state approach is linear in its parameters.  
996 We can thus compute the genotypic/breeding values in a given environment  $\varepsilon_k$  as

$$\mathcal{G}_z = \mathcal{A}_z = \hat{z} - E_{g|\varepsilon}(\hat{z}) = \boldsymbol{\mu}_g^T \mathbf{u}_k - \boldsymbol{\mu}^T \mathbf{u}_k = \mu_{g,k} - \mu_j, \quad (\text{S33})$$

997 where  $\mu_{g,k}$  and  $\mu_j$  are the  $k$ th values of the vectors  $\boldsymbol{\mu}_g$  and  $\boldsymbol{\mu}$ . The total (additive) genetic variance is the  
998 variance of the breeding values across environments:

$$V_{\text{Gen}} = V_{\text{Add}} = V(\mathcal{A}_z) = V(\mu_{g,k}). \quad (\text{S34})$$

999 Since the variance-covariance matrix of  $\boldsymbol{\mu}_g$  is the  $G_z$  matrix, the variance of all elements  $\mu_{g,k}$  taken together  
1000 is the average of the diagonal elements of  $G_z$ , which we will note  $V_k$ . Assuming that all environments are

---

<sup>88</sup>removed: in

1001 equiprobable for the sake of simplicity (releasing this assumption merely requires to use weighted average),  
 1002 we have

$$V_{\text{Add}} = \frac{1}{K} \sum_{k=1}^K V_k. \quad (\text{S35})$$

1003 In other words,  $V_{\text{Add}}$  is the average of the diagonal elements of the  $G_z$  matrix.

1004 The [<sup>89</sup>]environment-blind (additive) genetic variance of the trait depends on the average of the breeding  
 1005 values across environment for a given genotype:

$$\bar{\mathcal{A}} = \frac{1}{K} \sum_k \mathcal{A}_{z,k}, \quad (\text{S36})$$

1006 where  $\mathcal{A}_{z,k}$  is the breeding value evaluated at the  $k$ th environment for a given genotype, still assuming  
 1007 equiprobable environments. It results that the [<sup>90</sup>]environment-blind (additive) genetic variance of the  
 1008 trait is

$$V_G = V_A = \frac{1}{K^2} \left( \sum_k V_k + 2 \sum_{k<l} C_{kl} \right), \quad (\text{S37})$$

1009 where  $C_{kl}$  is the genetic covariance between the environment  $k$  and  $l$ . In other words,  $V_A$  is the average of all  
 1010 the elements of the  $G_z$  matrix.

1011 Finally, the (additive) genetic variance [<sup>91</sup>]arising from plasticity can be computed as the difference  
 1012 between  $V_{\text{Add}}$  and  $V_A$ :

$$V_{G \times E} = V_{A \times E} = V_{\text{Add}} - V_A = \frac{1}{K^2} \left( (K-1) \sum_k V_k - 2 \sum_{k<l} C_{kl} \right) \quad (\text{S38})$$

1013 A few particular cases are important to note here. The first case is when all environments harbour the  
 1014 same additive genetic variance, say  $V$ , and are all perfectly correlated with one another. This is a situation  
 1015 generally [<sup>92</sup>]describe as a total absence of genetic variation in plasticity. In our framework, this situation  
 1016 would indeed result in  $V_{\text{Add}} = V_A = V$  and, indeed, no genetic variation [<sup>93</sup>]arising from plasticity with  
 1017  $V_{A \times E} = 0$ . Note that uneven additive genetic variances across environments, even if genetic correlation  
 1018 are kept perfect across environments, would result in slightly positive genetic variance [<sup>94</sup>]arising from  
 1019 plasticity with  $V_{A \times E} > 0$ . This is because, in such context, the trait can still evolve faster in some environments  
 1020 compared to other, hence plasticity can evolve. The second extreme case, is when the [<sup>95</sup>]environment-  
 1021 blind additive genetic variance of the trait is null, i.e.  $V_A = 0$ , while all the additive genetic variance in

---

<sup>89</sup>removed: marginal

<sup>90</sup>removed: marginal

<sup>91</sup>removed: of

<sup>92</sup>removed: describe

<sup>93</sup>removed: in

<sup>94</sup>removed: in

<sup>95</sup>removed: marginal

1022 reaction norm is composed of the additive genetic variance [<sup>96</sup>] arising from plasticity, i.e.  $V_{\text{Add}} = V_{\text{A} \times \text{E}}$ . This  
 1023 happens when the sum of covariances (the total of which must be negative) exactly compensates the sum of  
 1024 diagonal variances in the  $G_z$ , meaning that [<sup>97</sup>] negative genetic correlation [<sup>98</sup>] between environments are  
 1025 maximised. In this case, it is impossible for directional selection to act on average value of the trait across  
 1026 all environments, but the evolvability of plasticity is [<sup>99</sup>] maximal. A third, interesting case is when there is  
 1027 absolutely no genetic correlation between environments, i.e. the off-diagonal elements of  $G_z$  are all equal to  
 1028 0. In such case, it is important to note that, because evolution can freely operate across environments, then  
 1029 both  $V_{\text{A}} = \frac{1}{K^2} \sum_k V_k$  and  $V_{\text{A} \times \text{E}} = \frac{K-1}{K^2} \sum_k V_k$  are non-zero.

## 1030 C5 Decomposition of variance for individual-based reaction norms

1031 In Equation 4, we assumed that the only source of variation in  $\theta$  is of genetic origin. This is a classical  
 1032 assumption both in the empirical and theoretical literature (de Jong 1990; Gavrillets & Scheiner 1993a; Via &  
 1033 Lande 1985), but in many cases, it can be useful or needed to include further sources of variation in  $\theta$ . This is  
 1034 for example the case when studying reaction norms using repeated measurements of the same individual in  
 1035 different environments. In particular, this may require including a further “permanent environment” effect  
 1036 to account for multiple repeats (Wilson et al. 2010) on the same individual, and also allows for the modelling  
 1037 of the reaction norm at the individual level (individual plasticity, Nussey et al. 2007). When other random  
 1038 effects are assumed in the model, we can write the full variation of  $\theta$  as:

$$\theta \sim \mathcal{N}(\bar{\theta}, V_{\theta}), \quad (\text{S39})$$

1039 where  $V_{\theta}$  is the total variance-covariance matrix of  $\theta$ . Note that Equation 4 is still valid to model the genetic  
 1040 component of  $\theta$  which we named  $\theta_g$ . In such case, the heritability of the  $k$ th component of  $\theta$  can be com-  
 1041 puted as the ratio of the  $k$ th diagonal element of  $G_{\theta}$  to the  $k$ th element of  $V_{\theta}$ , i.e.  $h_{\theta,k}^2 = \frac{G_{\theta,k,k}}{V_{\theta,k,k}}$ . Because the  
 1042 modelling of  $\theta_g$  remains unchanged, all our computations of (additive) genetic variances and their decompo-  
 1043 sition remains completely identical. However, there are two important changes. The first change is that the  
 1044 definition of  $V_{\text{Plas}}$  does not only depend on averaging over  $g$  any more, but on other sources of variations in  $\theta$   
 1045 as well, i.e.  $V_{\text{Plas}} = \text{V}(\text{E}_{\theta|\varepsilon}(\hat{z}))$ . This means that the marginalisation step conditional to the environment now  
 1046 implies the full  $V_{\theta}$  rather only its subcomponent  $G_{\theta}$ . The second change is that it is not possible to write the  
 1047 total variance of the reaction norm as the sum of  $V_{\text{Plas}}$  and  $V_{\text{Gen}}$  anymore, because the latter is only a partial  
 1048 reflection of the full variation in  $\theta$ . Instead, we need to introduce the phenotypic variation in the trait arising

<sup>96</sup>removed: in

<sup>97</sup>removed: strong

<sup>98</sup>removed: must exist between environments

<sup>99</sup>removed: maximised

1049 from the full sources of variation in  $\theta$ , which we denote here  $V_{\text{Param}}$ :

$$V_{\text{Param}} = V(\hat{z} - E_{\theta|\varepsilon}(\hat{z})) = E(V_{\theta|\varepsilon}(\hat{z})). \quad (\text{S40})$$

1050 Then, we can write the correct formulae for  $V_{\text{P}}$  and  $T_{\text{RN}}^2$ :

$$V_{\text{P}} = V_{\text{Plas}} + V_{\text{Param}} + V_{\text{Res}}, \quad T_{\text{RN}}^2 = \frac{V_{\text{Plas}} + V_{\text{Param}}}{V_{\text{P}}}. \quad (\text{S41})$$

1051 The Reacnorm package was designed to be able to input  $V_{\theta}$  to compute those quantities if needed.

## 1052 D Derivation of $\pi$ - and $\varphi$ -partition of $V_{\text{Plas}}$

### 1053 D1 The $\pi$ -decomposition

1054 We have seen in [Appendix C](#) how to compute the variance arising from the average shape of reaction norm  
 1055  $V_{\text{Plas}}$ . In order to go further, we now separate this into a component linked to the average slope of the reaction  
 1056 norm and another linked to the average curvature. For this, we need one or two of the following assumptions  
 1057 to hold true: (i) the environment  $\varepsilon$  follows a normal distribution; or (ii) the function  $f$  is quadratic. In such  
 1058 context, we can isolate the contribution of the slope,  $V_{\text{Sl}}$ , from the contribution of the curvature,  $V_{\text{Cv}}$  to  $V_{\text{Plas}}$ ,  
 1059 based on the best quadratic approximation of  $E_{g|\varepsilon}(\hat{z})$  (akin to the reasoning in Lande & Arnold 1983, for  
 1060 estimates of selection gradients), as:

$$V_{\text{Sl}} = E\left(\frac{dE_{g|\varepsilon}}{d\varepsilon}(\hat{z})\right)^2 V(\varepsilon), \quad V_{\text{Cv}} = \frac{1}{4}E\left(\frac{d^2E_{g|\varepsilon}}{d\varepsilon^2}(\hat{z})\right)^2 V(\varepsilon^2). \quad (\text{S42})$$

1061 As an illustration of why the assumptions above are needed, if  $\varepsilon$  follows a uniform distribution between -2  
 1062 and 2; and the average shape of plasticity is the following cubic function,  $f(\varepsilon) = 2\varepsilon - 0.5\varepsilon^2 - \varepsilon^3$ , then the  
 1063 average slope is -2, while the slope from the best quadratic approximation of  $E_{g|\varepsilon}(\hat{z})$  is -0.4. In such cases,  
 1064 the decomposition in [Equation S42](#) is not valid anymore, due to (i) the impossibility to apply Stein's lemma  
 1065 to a non-normal distribution and (ii) strong covariation between the slope and curvature. This means that  
 1066 whenever the environment is non-normal and the reaction norm is non-quadratic, the  $\pi$ -decomposition can  
 1067 bear little meaning (in the cubic example above,  $V_{\text{Sl}}$  would be 5.4, while  $V_{\text{Plas}} = 2.0$ , so that  $\pi_{\text{Sl}}$  would be largely  
 1068 above 1). A truly quadratic reaction norm is the only case where  $\pi_{\text{Sl}} + \pi_{\text{Cv}} = 1$ .

## 1069 D2 The $\varphi$ -decomposition

1070 In such cases where the environment is non-normal and the reaction norm is non-quadratic, it is always  
1071 possible to approximate the true shape of the reaction norm using a polynomial function:

$$\hat{z} = \sum_{n=0}^N (\bar{\theta}_n + \theta_{n,g}) \varepsilon^n \quad (\text{S43})$$

1072 In the context of decomposing  $V_{\text{Plas}}$ , such polynomial approximation provides a possibility to isolate the (co-  
1073 )contribution of the (pairs of) coefficients in  $E_{g|\varepsilon}(\hat{z}) = \sum_{n=0}^N \bar{\theta}_n \varepsilon^n$ :

$$V_{\text{Plas}} = V(E_{g|\varepsilon}(\hat{z})) = \sum_n \bar{\theta}_n^2 V(\varepsilon^n) + 2 \sum_{n < m} \bar{\theta}_n \bar{\theta}_m \text{cov}(\varepsilon^n, \varepsilon^m) \quad (\text{S44})$$

1074 From this, we suggest the alternative  $\varphi$ -decomposition of  $V_{\text{Plas}}$ , with  $\varphi_n = \frac{\bar{\theta}_n^2 V(\varepsilon^n)}{V_{\text{Plas}}}$  and  $\varphi_{nm} = \frac{2\bar{\theta}_n \bar{\theta}_m \text{cov}(\varepsilon^n, \varepsilon^m)}{V_{\text{Plas}}}$ .  
1075 It is important to note that this decomposition is based on the *coefficients* of the polynomial function and, thus,  
1076 it is unfortunately impossible to simply interpret the  $\varphi_n$  in terms of slope (for  $\varphi_1$ ), curvature (for  $\varphi_2$ ), and so  
1077 on. The only exception is when the reaction norm shape is quadratic, in which case  $\pi_{\text{Sl}} = \varphi_1$  and  $\pi_{\text{Cv}} = \varphi_2$ .

## 1078 E Correcting for uncertainty in the estimation of fixed 1079 effects

1080 **Character-state approach** It is easier to start with the character-state approach based on the ANOVA  
1081 model. We want to compute  $V_{\text{Plas}}$  as the variance of the group-level effects  $\mu$ :

$$V_{\text{Plas}} = V(\mu) \quad (\text{S45})$$

1082 However, we do not have access to the real-world values for  $\mu$ , but only to the estimated  $\hat{\mu}$  from the model.  
1083 Such estimates, if unbiased, have an expected value of  $\mu_k$  in environment  $k$  and a standard-error (i.e. the  
1084 estimation of the sampling standard deviation)  $s_k$ . In other words, we can state that  $\hat{\mu}_k$  is equal to  $\mu_k$  up to an  
1085 additive error:

$$\hat{\mu}_k = \mu_k + \tilde{\mu}_k \quad (\text{S46})$$

1086 where  $\tilde{\mu}$  is of mean 0 and variance  $s_k^2$ . Considering each virtual repeat  $r$  of the experiment, we can apply the  
1087 law of total variance:

$$V(\hat{\mu}) = V_\varepsilon(E_{r|\varepsilon}(\hat{\mu})) + E_\varepsilon(V_{r|\varepsilon}(\hat{\mu})) = V_\varepsilon(\mu) + E_\varepsilon(s^2). \quad (\text{S47})$$



1088 We thus have:

$$V_{\text{Plas}} = V_{\varepsilon}(\mu) = V_{\varepsilon}(\hat{\mu}) - E_{\varepsilon}(s^2) \quad (\text{S48})$$

1089 This result is equivalent to e.g. the classical computation of the “sire variance” in sire models in quantitative  
1090 genetics (Lynch & Walsh 1998), although the latter is generally expressed using sums-of-squares.

1091 **Curve-parameter approach** There is unfortunately no simple solution to the problem of accounting for  
1092 the uncertainty of fixed effects in the general context of non-linear modelling. However, for the particular  
1093 case where the model can be framed as a linear model, as is the case for the polynomial function, then  $\hat{z} = X\theta$ ,  
1094 where  $X$  is the design matrix containing the values for the environment. Noting  $\Sigma_X$  the variance-covariance  
1095 matrix of  $X$ , we can define  $V_{\text{Plas}}$  as:

$$V_{\text{Plas}} = \theta^T \Sigma_X \theta. \quad (\text{S49})$$

1096 Again, the problem is that  $\theta$  is unknown, we only have access to the estimated values of the parameters,  $\hat{\theta}$ ,  
1097 that are inferred with an error provided by the variance-covariance matrix of standard errors,  $S_{\theta}$ . We can  
1098 write again:

$$\hat{\theta} = \bar{\theta} + \tilde{\theta}, \quad (\text{S50})$$

1099 Noting that the error is independent from the true value, we have:

$$\hat{\theta}^T \Sigma_X \hat{\theta} = \theta^T \Sigma_X \theta + \tilde{\theta}^T \Sigma_X \tilde{\theta} \quad (\text{S51})$$

1100 To express  $\tilde{\theta}^T \Sigma_X \tilde{\theta}$ , it is important to note that  $S_{\theta,ij} = E(\tilde{\theta}_i \tilde{\theta}_j)$ , since  $E(\tilde{\theta}) = 0$ . Then, we can note that, the error  
1101 being unknown, we actually want to compute  $E_r(\tilde{\theta}^T \Sigma_X \tilde{\theta})$  taken across virtual repeats  $r$  of the experiment:

$$E_r(\tilde{\theta}^T \Sigma_X \tilde{\theta}) = E_r\left(\sum_{ij} \tilde{\theta}_i \tilde{\theta}_j \Sigma_{X,i,j}\right) = \sum_{ij} E_r(\tilde{\theta}_i \tilde{\theta}_j) \Sigma_{X,i,j} = \sum_{ij} S_{\theta,ij} \Sigma_{X,i,j} = \text{Tr}(S_{\theta} \Sigma_X) \quad (\text{S52})$$

1102 This is similar to the result of Brown & Rutemiller (1977). Finally, we have:

$$V_{\text{Plas}} = \hat{\theta}^T \Sigma_X \hat{\theta} - \text{Tr}(S_{\theta} \Sigma_X). \quad (\text{S53})$$

# 1103 F Full results for the section “Perfect modelling of quadratic 1104 curves”

1105 This section provides the full results corresponding to the section “Perfect modelling of quadratic curves” in  
1106 the main text. The results of all investigated values for the number of environments (10 or 4) and number of  
1107 genotypes (20 or 5 for the discrete case, 200 or 50 for the continuous case) are provided for the discrete and  
1108 continuous cases.

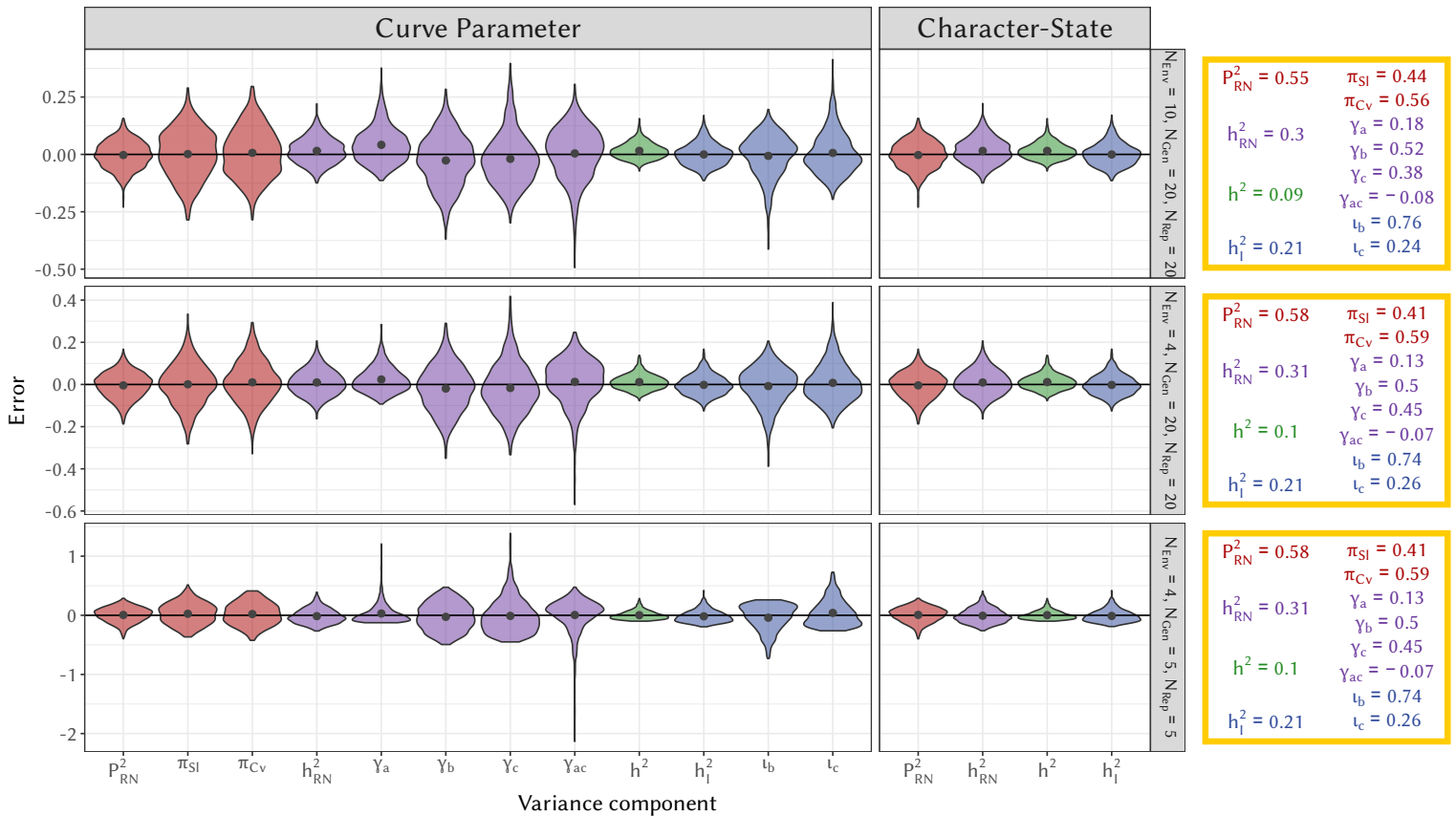


**Figure S1:** Distribution of the error (difference between the inferred and true value) for each the inferred variance components for three discrete scenarios:  $N_{env}$ : number of environments,  $N_{Gen}$ : number of different genotypes,  $N_{Rep}$ : number of replicates per genotype. Estimates are for  $\hat{P}_{RN}^2$  (proportion of variance generated by plasticity after averaging across genotypes),  $\hat{h}_{RN}^2$  (total heritability of the reaction norm),  $\hat{h}^2$  (environment-blind heritability[..<sup>a</sup> ]) and  $\hat{h}_1^2$  (heritability [..<sup>b</sup> ] from plasticity) for both the curve-parameter and character-state approaches. For the curve-parameter, the  $\pi$ -decomposition of  $\hat{P}_{RN}^2$  into  $\pi_{SI}$  (contribution of the slope) and  $\pi_{Cv}$  (contribution of the curvature); the  $\gamma$ -decomposition of  $\hat{h}_{RN}^2$  into  $\gamma_a$  (genetic contribution of the intercept),  $\gamma_b$  (genetic contribution of the slope),  $\gamma_c$  (genetic contribution of the curvature) and  $\gamma_{ac}$  (genetic contribution of the covariance between the intercept and the curvature) and the  $l$ -decomposition of  $\hat{h}_1^2$  into  $l_b$  (slope) and  $l_c$  (curvature) are also shown. The grey dots correspond to the average over the 1000 simulations.[..<sup>c</sup> ]

<sup>a</sup>removed: based on average breeding values

<sup>b</sup>removed: of

<sup>c</sup>removed: The effective number of dimensions  $n_e$  from the character-state is not shown, due to an important bias impacting the comparison with the other parameters.

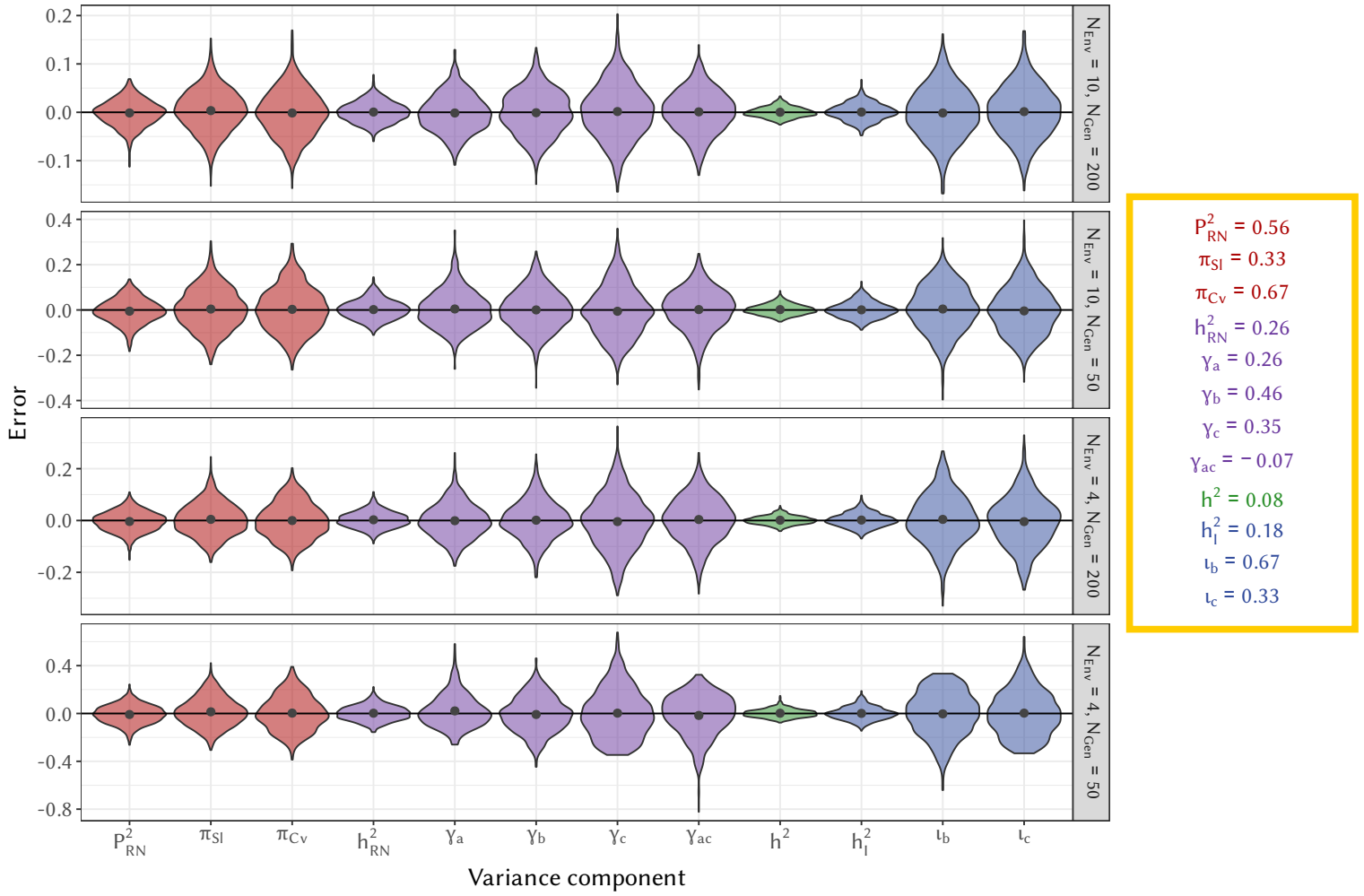


**Figure S2:** Distribution of the error (difference between the inferred and true value) for each the inferred variance components for four continuous scenarios:  $N_{env}$ : number of environment tested per genotype,  $N_{Gen}$ : number of different genotypes. The character-state approach was impossible for the continuous environment scenario. Estimates are for  $\hat{P}_{RN}^2$  (proportion of variance generated by plasticity after averaging across genotypes),  $\hat{h}_{RN}^2$  (total heritability of the reaction norm),  $\hat{h}^2$  (environment-blind heritability<sup>[.a]</sup>) and  $\hat{h}_l^2$  (heritability<sup>[.b]</sup> from plasticity) for both the curve-parameter and character-state approaches. For the curve-parameter, the  $\pi$ -decomposition of  $\hat{P}_{RN}^2$  into  $\pi_{SI}$  (contribution of the slope) and  $\pi_{Cv}$  (contribution of the curvature); the  $\gamma$ -decomposition of  $\hat{h}_{RN}^2$  into  $\gamma_a$  (genetic contribution of the intercept),  $\gamma_b$  (genetic contribution of the slope),  $\gamma_c$  (genetic contribution of the curvature) and  $\gamma_{ac}$  (genetic contribution of the covariance between the intercept and the curvature) and the  $l$ -decomposition of  $\hat{h}_l^2$  into  $l_b$  (slope) and  $l_c$  (curvature) are also shown. The grey dots correspond to the average over the 1000 simulations<sup>[.c]</sup>.

<sup>a</sup>removed: based on average breeding values

<sup>b</sup>removed: of

<sup>c</sup>removed: . The effective number of dimensions  $n_e$  from the character-state is not shown, due to an important bias impacting the comparison with the other parameters

## 1109 G Comparison with the approach from Murren *et al.* (2014)

1110 Murren *et al.* (2014) studied variation of the reaction norm shapes across different datasets, using their own  
 1111 metrics. We argue in the main text that our variance decomposition is more appropriate than the ones sug-  
 1112 gested by Murren *et al.* (2014), and we develop here why.

1113 The first step in the approach of Murren *et al.* (2014) is to choose a reference reaction norm in each of the

1114 studies and compute contrasts (i.e. difference with) to that particular reaction norm. The contrasts are then  
 1115 analysed, rather than the reaction norms themselves. For the sake of simplicity, and because this does not (or  
 1116 marginally) impact our comments on this approach, we will overlook that step and consider reaction norms  
 1117 directly.

1118 For each genotype  $k$  and from its given reaction norm (or contrast)  $z_k = \{z_{k,1}, \dots, z_{k,n}\}$ , Murren et al. (2014)  
 1119 compute four statistics (we removed the absolute values for the sake of simplicity here):

- 1120 1. The offset,  $O_M$ , measures the “location” of the reaction norm, i.e. its mean. Comparison of the offsets  
 1121 allows detecting whether reaction norms are “shifted” toward higher or lower values. It is computed, for  
 1122 each genotype  $k$ , as the absolute value of the average of the norm across environments:

$$O_{M,k} = \frac{\sum_i^n |z_{k,i}|}{n}. \quad (\text{S54})$$

- 1123 2. The slope,  $S_M$ , measures the linear trend of the reaction norms. Formally, it is the absolute sum of the  
 1124 differences between two consecutive environments, divided by the number of intervals ( $n - 1$ ):

$$S_{M,k} = \frac{\sum_i^{n-1} |z_{k,i+1} - z_{k,i}|}{n - 1}. \quad (\text{S55})$$

- 1125 3. The curvature,  $C_M$ , is computed as the absolute value of the average change in phenotype between two  
 1126 consecutive pairs of environments:

$$C_{M,k} = \frac{\sum_i^{n-2} |(z_{k,i+2} - z_{k,i+1}) - (z_{k,i+1} - z_{k,i})|}{n - 2}. \quad (\text{S56})$$

- 1127 4. The wiggle,  $W_M$ , is, according to the authors the “the variability in shape not described by any of the  
 1128 previous three measures”:

$$W_{M,k} = \frac{\sum_i^{n-2} |(z_{k,i+2} - z_{k,i+1}) - (z_{k,i+1} - z_{k,i})|}{n - 2} - C_{M,k}. \quad (\text{S57})$$

1129 Given the lower interest in this latter statistics, we will not comment on it any further. Most of the  
 1130 comments on the other statistics also apply to this one.

1131 One strong assumption underlying the calculations above is that environmental values  $\varepsilon = \{\varepsilon_1, \dots, \varepsilon_n\}$  on  
 1132 which the reaction norms were evaluated are evenly spaced, e.g. that the differences  $\varepsilon_{i+1} - \varepsilon_i$  are equal for  
 1133 all possible values of  $i$ . The assumption is actually that the space between two measures is equal to 1 (which,  
 1134 admittedly, is only a matter of rescaling when evenly-spaced values are already assumed). If this is the case,  
 1135 then there is indeed no loss in generality in using the number of components ( $n$ ,  $n - 1$  and  $n - 2$ ) rather than

1136 actual values of  $x$  in the denominator. Although it is common for studies on reaction norms to use evenly-  
 1137 spaced environmental values, it is an unnecessary assumption that shall not be satisfied by all studies.  
 1138 Second, developing the sums in  $S_M$  and  $C_M$  above show that the intermediate values cancel each other out,  
 1139 leaving only the values at each extreme of the environmental range in the estimate:

$$\begin{aligned}
 S_{M,k} &= \frac{z_{k,n} - z_{k,1}}{n - 1}, \\
 C_{M,k} &= \frac{(z_{k,n} - z_{k,n-1}) - (z_{k,2} - z_{k,1})}{n - 2}.
 \end{aligned}
 \tag{S58}$$

1140 The issue here is double: (i) the estimation is highly sensitive to the random noise coming from a small number  
 1141 of values (two or three/four); and (ii) the intermediate values in the reaction norm are simply thrown out and  
 1142 not used for a more robust estimation. In other words, it would have been exactly the same to not measure  
 1143 the reaction norm at these intermediate values, since they are not accounted for in the calculation.  
 1144 A final issue is that the approach uses the measured values of the reaction norms without accounting for the  
 1145 uncertainty in their estimation (i.e. standard-deviation and sample size for each genotype and environmental  
 1146 value) which poses the well-known issue of non-propagation of the error when doing “statistics on statistics”.

1147 Although we also provide estimators of the impact of several aspects of reaction norms on the phenotypic  
 1148 variation, our approach differs from the one from Murren *et al.* (2014) by many aspects. First, our variance  
 1149 decomposition makes the explicit distinction between the average shape of the reaction norm and the genetic  
 1150 variance surrounding it. As such, to  $O_M$ ,  $S_M$  and  $C_M$  corresponds not only the  $\pi$ -, but also the  $\gamma$ - and  $\iota$ -  
 1151 decomposition. We clearly delimit the domain of validity of each of these decomposition. We also account  
 1152 for possible correlation between those components. Second, we use the whole of the statistical inference to  
 1153 define our variance decomposition estimates. Third, we explicitly account for the uncertain estimation of  
 1154 reaction norms.